A set of methods to evaluate the below-cloud evaporation effect on local precipitation isotopic composition: a case study in Xi'an, China ~~A comparison of two methods to quantitatively evaluate the effect of below-cloud evaporation on the precipitation isotopic composition in the semi-arid region of the Chinese Loess Plateau~~

Meng Xing[1,2*], Weiguo Liu[1,2,3*], Jing Hu[1,2], Zheng Wang[1,2]

1.State Key Laboratory of Loess and Quaternary Geology, Institute of Earth Environment, Chinese Academy of Sciences, Xi'an, 710061, China

2.CAS Center for Excellence in Quaternary Science and Global Change, Xi'an, 710061, China.

3. University of Chinese Academy of Sciences, Beijing, 100049, China

Corresponding authors:

Meng Xing email address: xingmeng@ieecas.cn

Weiguo Liu email address: liuwg@loess.llqg.ac.cn

Abstract:

When the hydrometeor falls from the in-cloud saturated environment towards the ground, especially in the arid and semi-arid regions, the ~~Below~~below-cloud ~~evaporation effect~~processes could heavily alter the precipitation ~~isotope~~ isotopic composition ~~of the rain water as it travels from the saturated environment in the cloud towards the surface, especially in the arid and semi-arid regions~~through equilibrium and non-equilibrium fractionations, and accounts for the ~~misinterpreting~~ misinterpretation of ~~the~~ precipitation isotopic signal if these processes cannot be properly identified. To correctly understand the environmental information contained in the precipitation isotopes, qualitatively analyzing the below-cloud processes and quantitatively calculating the below-cloud evaporation effect are becoming very important ~~the first step is to qualitatively analyze the below-cloud processes that the raindrops have encountered during their falling, and then to quantitatively compute the below-cloud evaporation ratio of raindrops~~. Here, based on a two-year synchronous observations of precipitation and water vapor isotopes in Xi'an, we compiled a set of effective methods to systematically evaluate~~d~~ the below-cloud evaporation effect on local precipitation isotopic composition~~the variations of precipitation and water vapor isotopes caused by the below-cloud evaporation effect~~. ~~The precipitation $\delta^{18}O$ and $\delta^{2}H$ values range from -18.2‰ to 8.8‰ and -131.7‰ to 61.2‰, respectively, while the water vapor $\delta^{18}O_v$ and $\delta^{2}H_v$ values range from -29.5‰ to -10.1‰ and -214.9‰ to -63.9‰, respectively. Our results suggest that the equilibrium method could be successfully used to predict the ground-level water vapor isotopic composition from precipitation isotopes in semi-arid climates, especially for the winter data. Moreover, b~~The Δdδ-diagram shows the isotopic composition ($\delta^{2}H$, d-excess) of equilibrium vapor from precipitation samples relative to the ambient vapor, while equilibration and evaporation could lead to different pathways in the two-dimensional phase space of the Δdδ-diagram. By using Δdδ-diagram, our data show that evaporation is the ~~main~~ major below-cloud process of raindrops, while snowfall samples retain the initial cloud signal because of less isotopic exchange between vapor and solid phases. ~~In terms of meteorological factors, both temperature, relative humidity, and precipitation amount affect the intensity of below-cloud evaporation.~~ To quantitatively characterize the influence of below-cloud evaporation on precipitation isotopic composition, we chose two methods that one is based on the raindrop's mass change during its falling (hereafter referred to as method 1), and another directly calculate the precipitation isotopic variations from the cloud base to the ground (hereafter referred to as method 2). By comparison, the slope of evaporation proportion and difference in $\delta^{2}H$ ($F_i/\Delta\delta^{2}H$)

calculated by method 1 (1.0 ‰/%) is larger than method 2 (0.9 ‰/%). Additionally, both methods indicate that the raindrops are weakly evaporated in autumn, and heavily evaporated in spring ~~In arid and semi-arid regions, the below-cloud evaporation ratio computed by the mass conservation equation would be overestimated relative to the isotopic method, while~~. Through the sensitivity test relative humidity is the most sensitive parameter in both methods in ~~computing~~ deciding the below-cloud evaporation effect~~the remaining fraction of raindrop mass after evaporation~~. ~~In this study, the mean remaining fractions of raindrop mass calculated by the isotopic method respectively are 69.2%, 74.5%, 85.2%, and 80.8% in spring, summer, autumn, and winter. The raindrops are weakly evaporated in autumn and winter, and heavily evaporated in spring and summer.~~ Therefore, through following our methods, the diagnosis of below-cloud processes and the understanding of their effects on the precipitation isotopic composition will be improved.

~~Based on water vapor and precipitation isotope compositions, we designed a set of effective methods to evaluate the below-cloud evaporation effect, and this will improve our understanding of the information contained in the isotopic signals of precipitation~~.

1 Introduction

~~The hydrogen and oxygen isotopes of precipitation are one of the greatly important tools to trace the hydrological cycle and climate change (Bowen et al., 2019; Gat, 1996).~~ For the paleoenvironment, the isotopic signals of precipitation recorded in ice cores (Thompson et al., 2000; Yao et al., 1996), tree rings (Liu et al., 2004; Liu et al., 2017b), speleothems (Cai et al., 2010; Tan et al., 2014), and leaf wax of loess-paleosol deposits (Wang et al., 2018b) and lake sediments (Liu et al., 2017a, 2019) could be used to reconstruct the information of temperature, precipitation, and hydrological regimes in geologic history, as it had participated into the formation or the growth of these geological archives. For the modern environment, the isotopic ~~ratios~~ compositions of precipitation could be used to quantitatively constraint the water vapor contribution from the end-members of advection (Peng et al., 2011), evaporation (Sun et al., 2020; Wang et al., 2016a), transpiration (Li et al., 2016; Zhao et al., 2019), and even anthropogenic activities (Fiorella et al., 2018; Gorski et al., 2015; Xing et al., 2020), as itself is an important part of the hydrological cycle. Thus, the hydrogen and oxygen isotopes of precipitation are one of the most important tools to trace the hydrological cycle and climate change (Bowen et al., 2019; Gat, 1996). However, due to the limitations in sampling and isotopic fractionation theories, there remains large uncertainty (i.e., the ~~remaining fraction of~~ below-cloud evaporation intensity, the

moisture recycling ratio, water molecules exchange between the droplet and ambient air, etc.) in deciphering the information contained in precipitation by using hydrogen and oxygen isotope ~~ratios~~ compositions (Bowen et al., 2019; Yao et al., 2013).

~~Chinese Loess Plateau (CLP) is located in the arid and semi-arid areas, where many studies have suggested that the precipitation isotopic composition has been more or less impacted by the below-cloud evaporation and surface moisture recycling effects (Sun et al., 2020; Wan et al., 2018; Zhang and Wang, 2016). Therefore, before we utilize precipitation stable isotopes to reconstruct the climate changes or to trace the water vapor sources, first we need to have a set of reliable evaluation methods to diagnose whether the isotope ratios of precipitation have been distorted by the below-cloud evaporation effect (Graf et al., 2019; Wang et al., 2016b). Then, we need to quantitatively evaluate how much of the raindrops have been evaporated during their falling. Finally, we are able to use the original precipitation isotopes data, which have been calibrated by the below-cloud evaporation effect, to discuss the regional water vapor sources or the global hydrological cycle. At present, however, there are many efforts to do in the first and second steps.~~

Below-cloud evaporation is exactly one of the processes that influences the falling raindrops modifying their final stable isotopic content, and thus needs to be properly evaluated. Over the past decades, to determine whether the hydrometeor~~s~~ have been evaporated during ~~their~~its falling, most studies depend on a second-order isotopic parameter (Dansgaard, 1964; Jeelani et al., 2018; Li and Garzione, 2017), deuterium excess (defined as d-excess= $\delta^{2}H-8\times\delta^{18}O$). This parameter is representative of the non-equilibrium ~~kinetic~~ fractionations, since light isotopes (^{1}H and ^{16}O)~~$^{2}H^{1}H^{16}O$~~ equilibrate~~s~~ faster than heavy isotopes (^{2}H and ^{18}O) ~~$^{1}H_{2}^{18}O$~~ in different phases (Clark and Fritz, 1997; Dansgaard, 1964). ~~With both the equilibrium and kinetic effects~~For raindrops, the lighter ~~isotopes~~ water molecules ($^{1}H_{2}^{16}O$) ~~(^{1}H and ^{16}O) of raindrops~~ preferentially equilibrate or diffuse from the liquid phase to the gas phase during their falling through unsaturated ambient air, while the equilibrium fractionation would not change the d-excess ~~while~~ but the non-equilibrium diffusional process would result in a decrease of d-excess in rain (FISHER, 1991; Merlivat and Jouzel, 1979). ~~Correspondingly, the non-equilibrium evaporation effect would cause the increase of deuterium excess in the surrounding water vapor.~~ Additionally, ~~The~~ the slope of the local meteoric water line (LMWL) has also been widely used as a metric to infer the below-cloud evaporation effect according to the theory of water isotope equilibrium

fractionation (Chakraborty et al., 2016; Putman et al., 2019b; Wang et al., 2018a)~~.~~, ~~in which~~Generally, the LMWL's slope~~s~~ approximately equals to 8.0 belonging to equilibrium fractionation and that is lower than 8.0 pointing to a non-equilibrium fractionation, such as the re-evaporation of raindrops. ~~Nonetheless, it should be noted that a change of air masses (Guan et al., 2013), condensation in supersaturation conditions (Jouzel et al., 2013), and moisture exchange in the cloud and sub-cloud layer (Graf et al., 2019) also cause largely spatial variation in slopes and d-excess values (Putman et al., 2019a; Tian et al., 2018).~~

However, it ~~should be~~is worth noted~~ed~~ing that a~~t~~he change of air masses (Guan et al., 2013), the condensation in supersaturation conditions (Jouzel et al., 2013), and~~or~~ the moisture exchange in the cloud and sub-cloud layer (Graf et al., 2019) also cause large~~ly spatial~~ variations in the slopes and d-excess values (Putman et al., 2019a; Tian et al., 2018). Therefore, it is imperative to explore a novel method to more accurately identify the below-cloud evaporation. Recently, Graf et al. (2019) provided a new interpretive framework to directly separate the convoluted influences on the stable isotopic composition of vapor and precipitation according to the theoretical fractionation processes, especially the influences of equilibration and below-cloud evaporation. The axes of the new diagram consist of the differences, $\Delta\delta^2H$ and Δd, between the isotopic composition of equilibrium vapor from precipitation relative to near-surface vapor, namely $\Delta\delta\Delta d$-diagram. Compared with the slope of LMWL or the d-excess, the below-cloud equilibration and evaporation have different spatial distributions in the two-dimensional phase space of $\Delta\delta\Delta d$-diagram, which makes them more easily distinguishable. Although the $\Delta\delta\Delta d$-diagram gives us a new guideline to more accurately identify the below-cloud evaporation, Graf's et al. (2019) work was only tested on a cold frontal rain event during a short time, and hence more works need to be done for validating the general applicability of their framework.

~~Traditionally, extensive data on the isotopic content of the condensed phases (e.g., precipitation, snow, ice core, etc.) have been widely used to study the mechanisms of the atmospheric transport process of water vapor and the subsequent phase changes in the atmosphere. Inevitably, important information will lose by using the isotopic composition of the liquid or solid water samples only. As an improvement, simultaneous observations of water vapor and precipitation are applied to distinguish these processes and quantify below-cloud processes. For example, Yu et al. (2015, 2016) used a custom-made sampling device to collect daily water vapor samples over~~

the Tibetan and Pamir Plateau, and discussed moisture source impacts on the precipitation isotopes. Using a three-stage Caltech Active Strand Cloud water Collector (CASCC), Spiegel et al. (2012b, 2012a) investigated the impact of different processes within clouds, and found that the origin of the water vapor forming near-surface clouds (fog) is key in determining the temporal evolution of cloud water isotopes. With the aid of the off-line water vapor sampling system, Deshpande et al. (2010) analyzed the rain-vapor interaction using stable isotopes. However, the old water vapor cryogenic trapping technique is time-consuming (Christner et al., 2018), labor-intensive (Welp et al., 2012), and discrete (Wen et al., 2016), limiting the further examination of the two-phase system.

In recent years, with the progress in optical laser systems, the relatively portable field-deployable laser spectroscopic instruments, simultaneously measuring $^{1}H_{2}^{16}O$, $^{2}H^{1}H^{16}O$, and $^{1}H_{2}^{18}O$ isotopes, allows performing online, autonomous, and long-term site measurements of the water vapor stable isotope composition (Aemisegger et al., 2012; Christner et al., 2018). The emergence of this instrument exerts a great impact on the study of water vapor isotopic composition, leading to a substantially increased number of observations in near-ground water vapor, while the interpretation of water vapor isotopic data has the potential to deepen our cognition in water vapor isotopic variations and fractionation processes during the two-phase transformation (Noone et al., 2011; Steen-Larsen et al., 2014). Wen et al. (2010) first analyzed the d-excess$_{vap}$ (denotes the d-excess of water vapor) at hourly temporal resolution in Beijing, China, and systematically discussed the controls on the isotopic exchange between vapor and condensed phase. Griffis et al. (2016) used multi-year water vapor and precipitation stable isotope results to evaluate the water vapor contributions to the planetary boundary layer from evaporation in Minnesota, United States. Laskar et al. (2014) and Rangarajan et al. (2017) comprehensively investigated the water vapor sources and raindrop-vapor interaction in Taibei, and developed a box model to explain the controlling factors for high and low d-excess$_{vap}$ events in this region. Combined with observations and numerical simulations of stable isotopes in vapor and rain impacted by cold fronts, Aemisegger et al. (2015) clearly revealed the importance of below-cloud processes for improving the simulations. An overview of the increasing number of available water vapor isotope observations can be found in Wei et al. (2019). As a creative work, Graf et al. (2019) introduced a new interpretive framework to directly separate the convoluted influences on the stable isotopic composition of vapor and precipitation according to the theoretical fractionation processes, especially the

~~influences of equilibration and below-cloud evaporation, which enables us to disentangle the governing below-cloud processes in the course of a rainfall. Although Graf's et al. (2019) work gives us a new guideline to more accurately judge the raindrops experienced below-cloud evaporation effect, their work was only validated on a cold frontal rain event of a short period, and hence more works need to do for proving the general applicability of their framework.~~

~~In order to get t~~The initial signal of precipitation isotopes is important in hydrological studies, and thus it is necessary to quantitatively ~~assess~~ estimate the impact of below-cloud evaporation on ~~the~~its variations ~~stable isotopes~~. Generally, the difference between the isotopic composition of precipitation in the ground level and cloud base is determined by the below-cloud evaporation effect. Because it is difficult to measure the vapor or precipitation isotopic composition at the cloud base, the model proposed by Stewart (1975) has been widely used to estimation of the below-cloud evaporation effect on the precipitation isotopic composition for a long time. Based on the well-defined laboratory conditions, Stewart (1975) parameterized the change of the isotopic composition of a falling water drop with the vapor and raindrop isotopic compositions at the cloud base, and the remaining fraction of raindrop mass after evaporation (hereafter referred to as method 1). Froehlich et al. (Froehlich et al., 2008) adapted the Stewart model and then assessed the change in d-excess due to below-cloud evaporation based on a simple frame in the European Alps. Wang et al. (2016b) further refined the calculations of the parameters, which are used to determine the remaining fraction of raindrop mass in the Stewart model, to assess the variation in d-excess of raindrops in central Asia. However, the quantitative evaluation of below-cloud evaporation effect which is based on Stewart model is indirect, because the result is largely dependent on the parameter that the remaining fraction of raindrop mass after evaporation.

In recent years, with the progress in optical laser systems, a relatively portable field-deployable laser spectroscopic instruments have emerged, which makes the online, autonomous, and high-frequency site measurements of the water vapor stable isotope composition be achieved (Aemisegger et al., 2012; Christner et al., 2018). Therefore, the vapor or precipitation isotopic composition at the cloud base could be directly measured (Salmon et al., 2019), or indirectly deduced from the measurements of ground-level water vapor isotopic composition (Deshpande et al., 2010; Salamalikis et al., 2016). This enables us to directly calculate the difference between the isotopic

composition of precipitation in the ground level and cloud base (hereafter referred to as method 2). However, less work has systematically compared the differences of the computed results by these two methods on below-cloud evaporation effect.

~~The model suggested by Stewart (1975) has been widely used to calculate the below-cloud evaporation ratio of raindrops, as the raindrops experienced physical processes have been explicitly described by this isotope-evaporation model (Müller et al., 2017; Sun et al., 2020; Zhao et al., 2019). Based on Stewart's (1975) work, the remaining fraction of raindrop mass (F_r) after evaporation could be calculated according to the differences between the stable isotope ratios in collected precipitation near the ground and below the cloud base (See Data and Methods, section 2.3.2, eq 7). We note that some of the studies used the mass conservation model of a falling raindrop to calculate F_r (See Data and Methods, section 2.3.3, eq 8; Kong et al., 2013; Li et al., 2016; Sun et al., 2019; Wang et al., 2016b), and some of the works assumed the F_r is a constant (Müller et al., 2017), but no work has been reported by using ground-based and cloud-based observations of water vapor isotopes to calculate the F_r according to our knowledge. Due to the numerous uncertainty of the parameters in the mass conservation model, such as the factors of terminal velocity, the evaporation intensity, and the diameter of the raindrops, the error propagation will largely raise the deviation of F_r in the model. So far, no work has systematically evaluated the differences of F_r computed by the observed isotope results and the classical mass conservation model.~~

Here, we ~~have measured~~use the measurements of ~~the~~ two-year near-ground water vapor isotope composition ~~composition in Xi'an city (34.23°N, 108.88°E), Shaanxi province, located in the CLP~~, ~~for 2 years, while~~ and 141 precipitation ~~collecting~~ isotope compositions ~~141 precipitation samples~~ (including event-based snowfall samples)~~.~~which were collected in Xi'an (34.23°N, 108.88°E), Shaanxi province, located in the Chinese Loess Plateau (CLP). The objectives of this study are to: 1. qualitatively identify the below-cloud processes of falling raindrops by using the Δδ-Δd-diagram ~~test the applicability of the Δd-Δδ-diagram suggested by Graf et al. (2019) when it is used to diagnose the below-cloud processes for our dataset~~; 2. quantitatively evaluate the below-cloud evaporation effect on precipitation isotopic composition by two methods and compare their differences~~compare the differences of raindrops below-cloud evaporation ratio calculated by the observed ground-based water vapor isotope composition and the mass conservation model~~; 3. understand the role of main meteorological factors, such as temperature, relative humidity (RH), and precipitation

amount, on the below-cloud evaporation effect, and the seasonal variations of ~~below-cloud~~ evaporation proportion~~ratio~~ in CLP. Therefore, ~~With~~ with the advantages of the paired observations of the vapor and precipitation in stable isotopes near the ground level, this study will compile a set of effective methods ~~provide a new set of methods~~ to ~~determine~~ evaluate the below-cloud evaporation effect on the local precipitation isotopic composition. ~~Therefore, our insight into the below-cloud evaporation effect on the isotopic composition of precipitation in arid and semi-arid areas would be deepened and strengthened.~~

2 Data and methods

2.1 Sampling site

As the capital city of Shaanxi province and the largest city in northwest China, Xi'an is located on the Guanzhong Plain on the southern edge of the CLP at an average elevation of 400 m. The city is located in a semi-arid to arid region and is representative of most cities in the north and northwest of China (e.g., Lanzhou and Xining city, Fig. 1). The mean annual precipitation is 573.7mm, and the mean annual evaporation is 426.6mm from 1951 to 2008 year (Wu et al., 2013). The notable below-cloud evaporation effect has been reported ~~by~~ in many studies ~~in~~ for this area (Sun et al., 2020; Wan et al., 2018; Zhu et al., 2016). Therefore, it is an ideal area to study the below-cloud evaporation effect.

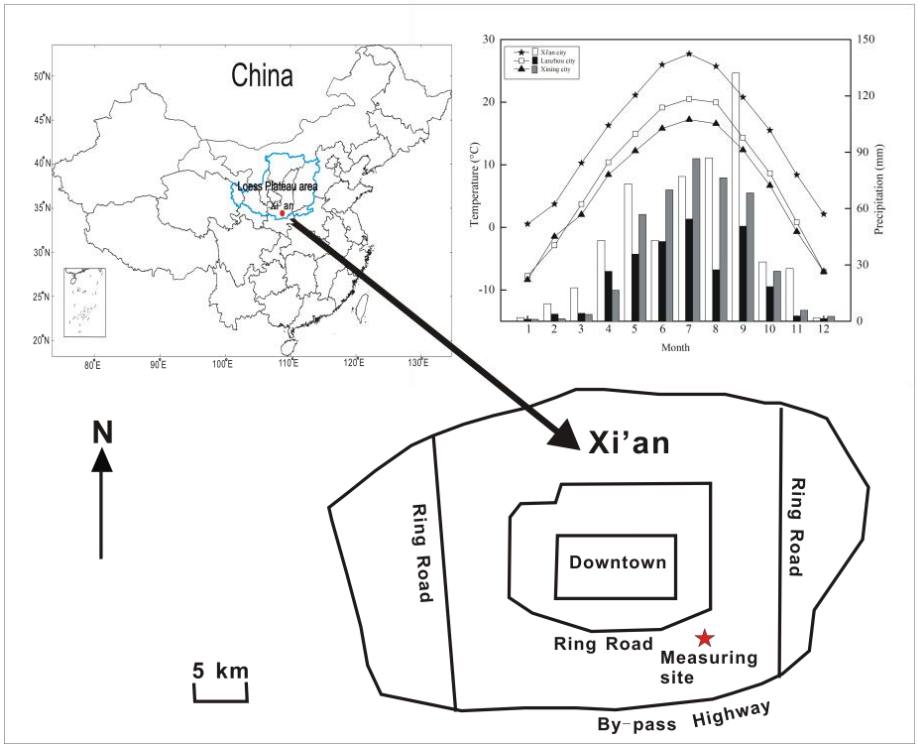

Figure 1 Average monthly variations of temperature and precipitation in Xi'an, Lanzhou, and Xining during 2010-2015. Location of the sampling site in the Yanta Zone, 9 km SE of downtown Xi'an. Water vapor samples are taken on the seventh floor of a twelve-story building, about 30 m above ground level. Precipitation samples are collected on the top floor, 1 m above ground level.

The water vapor in-situ measurement site is located in a residential area, approximately 10 km southeast to downtown of Xi'an city (Fig. 1). The atmospheric water vapor isotopic composition was observed from 1 January 2016 to 31 December 2017 on the seventh floor of the Institute of Earth and Environment, Chinese Academy of Sciences, about 30 m above ground level. The rainfall or snowfall collector was placed on the rooftop of the buildings (1 m above the floor of the roof), about 50 m above ground level .

2.2 Sampling and isotopic measurement

Rainfall and snowfall samples were collected manually from the beginning of each precipitation event using a polyethylene collector (700 mm × 450 mm × 170 mm) ~~and the volume was measured using a graduated flask~~. Before being used, the collector was cleaned with soap and water, rinsed with deionized water, and then dried. When the precipitation events end, the collector was quickly taken back to minimize water evaporation. The rainfall volume was measured using a graduated flask. After collection, the samples were filtered through 0.40–μm polycarbonate membranes. Then, ~~R~~the rainfall samples were immediately poured into a 100 ml polyethylene bottle. The snowfall samples were first melted at room temperature in a closed plastic bag ~~after collection~~, after filtration, and then immediately poured into a 100 ml polyethylene bottle. ~~After collection, samples were filtered through 0.40–μm polycarbonate membranes.~~ About a 2 ml of each filtrate was transferred into a sample vial, and stored at -4°C until being measured. Of the collected 141 samples, during the two-year sampling campaigns, ~~we collected~~ 130 are rainfall samples and other 11 are snowfall samples (Table S1).

In all cases, the data are reported in the standard delta notation (δ), i.e., the per mil (‰) deviation from Vienna Standard Mean Ocean Water according to, $\delta = (R_{sample}/R_{reference}-1) \times 1000$, where R is the isotope ratio of the heavy and light isotope (e.g., $^{18}O/^{16}O$) in the sample and the reference.

The precipitation samples were measured ~~by~~ with a Picarro L2130-i (serial number HIDS 2104) wavelength-scanned cavity ring-down spectrometer at a high-precision

mode~~l~~. Every isotopic standard or sample was injected sequentially 8 times using a 5 μL syringe, and then the arithmetic average of the last 3 injections was accepted as the final result. ~~The precision is better than 0.2‰ and 1.0‰ for $\delta^{18}O$ and $\delta^{2}H$, respectively.~~ All the samples were calibrated by three laboratory standards, while the $\delta^{18}O$ and $\delta^{2}H$ true values of the three laboratory standards (Laboratory Standard-1 (LS-1): $\delta^{18}O$ =+0.3‰, $\delta^{2}H$ =–0.4‰; Laboratory Standard-2 (LS-2): $\delta^{18}O$ =–8.8‰, $\delta^{2}H$ =–64.8‰; Laboratory Standard-3 (LS-3): $\delta^{18}O$ =–24.5‰, $\delta^{2}H$ =–189.1‰) are calibrated to the scale of two international standard material VSMOW-GISP, with a precision of ±0.2‰ and ±1.0‰, for $\delta^{18}O$ and $\delta^{2}H$, respectively. To correct the intrument drift, the three laboratory standards were repeatedly measured after measuring every 8 samples.

Atmospheric water vapor $\delta^{18}O_v$ and $\delta^{2}H_v$ were also measured by Picarro L2130-i ~~(serial number HIDS-2104)~~, but at a liquid-vapor dual model. The inlet of the gas-phase instrument is connected to the vapor source through an external solenoid valve when measuring vapor samples. This valve can switch the input of the instrument from the vapor sample to dry gas. The instrument is connected to dry gas prior to being connected to the evaporator for measuring liquid water standards so that any traces of the water vapor sample are removed from the measurement cell. The standards are injected into the evaporator and measured by a CTC Analytics autosampler, PAL HTC-xt (Leap Technologies, Carrboro, NC, USA). The atmospheric water vapor is pumped through a 2m stainless-steel tube (1/8 inch) using a diaphragm pump at the speed of 4 L min^{-1} and detected by the laser spectrometer. The outside length of the stainless-steel tube is about 0.5m, and the inside length is about 1.5m. We covered the stainless-steel tube with a heating tape maintained at 60°C to prevent water vapor from condensing in the stainless-steel tube. The air intake was protected with a shield to prevent rainwater from entering the sample line and direct sunlight.

The raw water vapor $\delta^{18}O_v$ and $\delta^{2}H_v$ data were obtained approximately at 1 Hz and then block-averaged into ~~24~~ 1 h intervals. As the main usage of this instrument is to measure the liquid water samples in our laboratory, it is used to monitor the water vapor isotopes in its spare time. Thus, the missing data ~~gaps represent~~ indicate that the instrument is used for ~~in liquid samples~~ measuring liquid samples ~~status~~ or being ~~maintenance~~maintained. The ~~daily average of~~event-based water vapor isotopic composition is the average value from ~~8:00 - 20:00 UTC (0:00 – 24:00 for local time)~~ the start of precipitation event to the end. ~~The average intra-day variability of water~~

~~vapor isotopic composition is less than 1.2‰ for $\delta^{18}O$ and 8.4‰ for $\delta^{2}H$ for two-year data, respectively, and on the precipitation day is 1.4‰ for $\delta^{18}O$ and 10.5‰ for $\delta^{2}H$, respectively.~~

The hourly meteorological data, such as temperature~~,~~ ~~and~~ RH, and surface pressure in Xi'an, are reported by the ~~China~~ Chinese meteorological administration, and can be downloaded from the website of http://www.weather.com.cn/. The meteorological station is about 10 km to the north of our sampling site.

~~Here, we need to note the different sampling frequencies between Graf's et al., (2019) and our study. To explicitly capture the below-cloud processes of the droplet, Graf's et al., (2019) study used the intra-event samples, which clearly record the equilibration, evaporation, and cloud signal on the ΔdΔδ-diagram. Particularly, the below-cloud evaporation effect does not accompany the entire rainfall process, for example, in the pre-frontal phase, the rain intensity and relative humidity are lower than in the post-frontal period, which causes the raindrops to be more strongly affected by below-cloud processes (Graf et al., 2019). In this study, we aim to quantitatively evaluate the evaporated degree of droplets in a single rain event, and compare the results of two different methods for calculating the remaining fraction of raindrop mass after evaporation. The per-event isotopic composition of precipitation is an integrated, mass-weighted average of the composition of all drops contained in a sample (Graf et al., 2019). The processes that act on a single drop are thus directly relevant for bulk precipitation. In the per-event sample, the offset between the precipitation equilibrated isotope ratios and the simultaneously observed isotope ratios of surface vapor can aid in inferring the below-cloud processes (Conroy et al., 2016). Hence, we chose the per-event samples as our study objects. Note that, the per-event samples whose isotopic results do not project on the fourth quadrant of ΔdΔδ-diagram, do not indicate the absence of below-cloud evaporation. It rather is an indication that the equilibration or the cloud isotopic signals dominate the mass-weighted isotopic composition of all drops.~~

2.3 The representativeness of the data

In 2 years, a total of 514 days of water vapor isotopic composition measurements were carried out. For 141 precipitation samples,of which 100 precipitation samples have corresponding event-based water vapor isotopic results. In this study, the precipitation events mainly occurred in summer and autumn, and less in winter and spring. In summer and autumn, the rainfall amount accounted for more than 70% of the annual

rainfall (Fig. S2). This is consistent with the multi-year average precipitation distribution in Xi'an (Fig. 1). Therefore, the samples we collected are representative of the precipitation characteristics in this region.

2.~~3~~ 4 Water vapor isotopic data ~~calibration~~correction

~~Due to~~Since the water vapor concentration effect and isotopic composition dependency ~~the isotopic measurements~~ of the cavity ringdown spectrometer ~~with water vapor concentration effect as~~has been ~~outlined~~ pointed out by ~~some~~ many studies (e.g., Bastrikov et al., 2014; Benetti et al., 2014; Steen-Larsen et al., 2013; Weng et al., 2020), it is important to determine the ~~humidity-isotope~~isotopic composition-humidity ~~calibration~~ corretion response function. ~~Because we did not have the Standards Delivery Module (Picarro) system or equivalent, the humidity calibration is based on data obtained from discrete injections of three known liquid standards with a PAL autosampler and the Picarro vaporizer unit (Benetti et al., 2014; Noone et al., 2013). The analyzer is programmed to perform a self-calibration after every 24 hours of ambient air measurement using an autosampler to inject liquid standards for producing different humidity. Injections were arranged at humidity levels near 3000, 5000, 8000, 10000, 15000, 20000, 25000, and 30000 ppm. Each reference sample is measured continuously for 8 times at one humidity level, and the last 3 times results were used to calculate the average to be recognized as the δ-value at the measured humidity. The humidity correction is the difference between the δ-value at the measurement humidity and the δ-value at a reference value taken as humidity = 20000 ppm.~~ The humidity dependency as shown in Fig. S1 also shows a dependency on the isotopic composition of the standards as reported by Weng et al. (2020). For example, in Figure S1a and Figure S1b, LS-1 shows a decrease in $\Delta\delta^{18}O$ and $\Delta\delta^{2}H$ with decreasing humidity while LS-3 shows an increase with decreasing humidity. Therefore, we referred the Weng's et al. (2020) correction sheme for this isotope composition-humidity dependency.

~~The best fit was reached with an exponential function for $\delta^{18}O_v$ and a linear function for $\delta^{2}H_v$ (Fig. S1a and S1b).~~ The isotopic measurements of ground-level $\delta^{18}O_v$ and $\delta^{2}H_v$ samples were corrected for ~~isotope~~ isotopic composition-humidity dependency using:

$$\delta_{measured} - \delta_{iso\text{-}hum\text{-}cor} = \frac{a(\delta_{iso\text{-}hum\text{-}cor})}{h} + b(\delta_{iso\text{-}hum\text{-}cor}) \times h + c(\delta_{iso\text{-}hum\text{-}cor}) \quad \text{(eq 1)}$$

~~$$\delta^{18}O_{humidity\ calibration} = \delta^{18}O_{measured} - (-4.91 \times e^{(-3.51 \times Measured\ humidity)}) \quad \text{(eq 1)}$$~~

~~and for ambient air $\delta^{2}H_v$ humidity correction using:~~

~~$$\delta^{2}H_{humidity\ calibration} = \delta^{2}H_{measured} - (0.0001 \times Measured\ humidity - 1.86) \quad \text{(eq 2)}$$~~

where $\delta_{iso\text{-}hum\text{-}cor}$$\delta_{humidity\ calibration}$ is the ~~calibrated data for~~corrected water vapor isotopic composition at 20000 ppmv~~vapor stable isotope~~; $\delta_{measured}$ is the raw, measured isotopic composition at that humidity~~data before calibration~~; ~~and measured humidity~~h is the ~~corresponding humidity at the time of measurement~~measure humidity; and a, b, and c are fitting coefficients for each water standard and isotope species. The detailed correction processes are provided in the supplementary material Appendix A.

To calibrate the measured water vapor isotopic composition to the VSMOW-GISP scale, three known-value laboratory standards have been used in the conversion, while these standards were measured in 24 h intervals to correct for instrument drifts. ~~The detailed post-calibration procedure is given in Xing et al. (2020).~~ The 1σ estimated total uncertainties are from 2.1 to 12.4 ‰ for δ^2H_v, 0.4 to 1.7 ‰ for $\delta^{18}O_v$, and 3.8 to 18.4 ‰ for d-excess$_v$ over the range of humidity from 30000 to 3000 ppmv on a 10-minutes average through the approach using a Monte Carlo method.

~~**2.4 The representative of the data**~~

~~During the two year study, we collected the precipitation samples for each event. Precipitation samples are generally collected from the beginning of the rainfall to the end. If the rainfall event exceeds 24 hours, we replace a sample collector at 8 am as a new precipitation sample. For the observation of water vapor isotopic composition, it has been done in the instrument's spare time, that is when the instrument is not on liquid water samples testing mission or maintaining status. In 2 years, a total of 514 days of water vapor isotopic composition were carried out, of which 100 precipitation samples have corresponding daily average water vapor isotopic results. In this study, the precipitation events mainly occurred in summer and autumn, and less in winter and spring. The rainfall amount accounted for more than 70% of the annual rainfall in summer and autumn (Fig. S2). This is consistent with the multi-year average precipitation distribution in Xi'an (Fig. 1). Therefore, the samples we collected are representative of the precipitation characteristics of this region.~~

2.5 Analytical methods

2.5.1 ΔdΔδ-diagram

As the raindrop is falling from the cloud base to the ground, it continuously exchanges with the surrounding vapor, but may lead to net loss as evaporation. However, this process is very hard to be quantified by observation. Using stable water isotopes, Graf et al. (2019) introduced a ΔdΔδ-diagram to diagnose below-cloud processes and their

effects on the isotopic composition of vapor and rain since equilibration and evaporation are two ~~various~~ different below-cloud processes and lead to different directions in the two-dimensional phase space of the ΔdΔδ-diagram. Here, the differences of isotopic composition of equilibrium vapor ($\delta^{18}O_{pv\text{-}eq}$, $d\text{-}excess_{pv\text{-}eq}$) from precipitation samples relative to the observed ground-based water vapor ($\delta^{18}O_{gr\text{-}v}$, $d\text{-}excess_{gr\text{-}v}$) can be expressed as:

$$\Delta\delta=\delta_{pv\text{-}eq}-\delta_{gr\text{-}v} \quad \text{(eq23)}$$

$$\Delta d\text{-}excess_v=d\text{-}excess_{pv\text{-}eq}-d\text{-}excess_{gr\text{-}v} \quad \text{(eq34)}$$

where $\delta_{pv\text{-}eq}$ and $\delta_{gr\text{-}v}$ are the δ^2H ($\delta^{18}O$) of equilibrium vapor from precipitation ~~water vapor below the cloud base~~ and ambient vapor near the ground, respectively, and $d\text{-}excess_{pv\text{-}eq}$ and $d\text{-}excess_{pv\text{-}eq}$~~gr-v~~ are d-excess values of equilibrium vapor from precipitation~~water vapor below the cloud base~~ and ambient vapor near the ground, respectively. For the detailed calculation processes, please refer to the supplemental material (Appendix X), or Graf et al. (2019).

~~To calculate the water vapor isotopic composition below the cloud base, we hypothesize the constant exchange of water molecules between the liquid and the vapor phases during the falling of raindrops, and the isotopic compositions reach towards equilibrium in the two phases during the processes. In the equilibrium state, the isotopic fractionation between the liquid and vapor phases follows a temperature-dependent factor:~~

~~$$\alpha=\frac{R_{pv\text{-}eq}}{R_p} \quad \text{(eq5)}$$~~

~~where $R_{pv\text{-}eq}$ is the water vapor isotope ratio between heavy and light isotopes ($^2H/^1H$ and $^{18}O/^{16}O$), R_p is the isotope ratio in precipitation, and α is a temperature-dependent equilibrium fractionation factor. Here, when the temperature is greater than 0 °C, we use the equation of Horita and Wesolowski (1994) to calculate $^2\alpha$ and $^{18}\alpha$, when the temperature is below 0 °C, the equilibrium fractionation factor proposed by Ellehoj et al. (2013) is used.~~

~~The above equation can be converted into δ-notation as:~~

~~$$\delta_{pv\text{-}eq}=\frac{1}{\alpha}(\delta_p+1000)-1000 \quad \text{(eq6)}$$~~

~~where δ_p is the isotope ratio in precipitation.~~

2.5.2 Below-cloud evaporation ~~calculated~~ calculation: Method 1 ~~by isotope~~

As reported by Stewart (1975), the isotopic composition of a falling water drop is:

$$^{i}R_{gr} = {}^{i}\gamma{}^{i}R_{va} + ({}^{i}R_{cb} - {}^{i}\gamma{}^{i}R_{va})F_r^{\,i\beta} \quad \text{(eq 5)}$$

where $^{i}R_{gr}$ is the isotopic ratio of falling raindrops near ground; $^{i}R_{va}$ and $^{i}R_{va}$ are the initial isotopic ratios for the vapor and raindrop at the cloud base; $^{i}\gamma$ and $^{i}\beta$ are the parameters related to the equilibrium fractionation factor, the relative humidity and the molecular diffusivities; and F_r is the remaining raindrop mass fraction after evaporation.

Assuming that the initial isotopic composition of the raindrop at cloud base is in equilibrium with the surrounding water vapor, Froehlich et al. (2008) adapted the Stewart model and simplified the equation to evaluate the isotopic enrichment due to below-cloud evaporation by:

~~suggested the falling raindrop isotopic fractionation of evaporation could be calculated according to the fraction of raindrop mass remained after evaporation:~~

$$\Delta\delta_p\delta = \delta_p - \delta_{zp\text{-}eq} = (1 - \frac{\gamma}{\alpha})(F_{iso}^{\beta} - 1) \quad \text{(eq67)}$$

$$F_i = (1\text{-}F_r) \times 100\% \quad \text{(eq 7)}$$

where δ_p and $\delta_{zp\text{-}eq}$ are precipitation isotope ratio near the ground and below the cloud base, respectively; F_{iso} is the remaining fraction of raindrop mass after evaporation (hereafter, the remaining fraction of raindrop mass calculated by this method is denoted as F_{iso}); α is equilibrium fractionation factor for hydrogen and oxygen isotopes; the parameters of γ and βγ and β is are defined by Stewart (1975); F_r is the remaining raindrop mass fraction after evaporation; and Δδ is the raindrop isotopic variations due to below-cloud evaporation; and F_i is evaporation proportion. For the detailed calculation processes, please refer to the supplemental material (Appendix XXA), or Froehlich et al. (2008), Wang et al. (2016b), and Salamalikis (2016), ~~Graf et al. (2019), and Sun et al. (2020)~~.

2.5.3 Below-cloud evaporation calculation: Method 2~~ed by mass conservation model~~

Because the isotopic composition of raindrop is directly influenced by the evaporation process during its falling, the below-cloud evaporation effect could be directly represented by the difference between the isotopic composition of precipitation in the ground level and cloud base:

$$\Delta\delta_p = \delta_{gr\text{-}p} - \delta_{cb\text{-}p} \quad \text{(eq 8)}$$

where $\delta_{gr\text{-}p}$ and $\delta_{cb\text{-}p}$ are the isotope compositions of a falling raindrop near ground and below cloud base, respectively; and Δδ is the raindrop isotopic variations due to below-

cloud evaporation. The $\delta_{gr\text{-}p}$ is our observed precipitation isotopic composition at Xi'an city, and $\delta_{cb\text{-}p}$ is calculated according to Deshpande et al. (2010). For the detailed calculation processes, please refer to the supplemental material (Appendix XX), or Araguás-Araguás et al. (2000), Deshpande et al. (2010), and Salamalikis (2016).

Actually, the method 1 is to evaluate the below-cloud evaporation effect on precipitation isotopic composition by calculating the mass change of the falling raindrop, while the method 2 is to directly calculate its effect on the isotopes.

~~Before the advent of the laser-based spectrometer, the water vapor isotopic composition measurement is labor-intensive and time-consuming, generally using the custom-made cold trap to collect. Normally, its observation is not a routine option. Therefore, to correct the measured δ/d-excess in precipitation (eq7) for the effect of below-cloud evaporation (Kong et al., 2013; Li et al., 2016a; Zhao et al., 2019) or study the differences and controls on δ/d-excess in precipitation caused by the below-cloud evaporation (Wang et al., 2016b), the Stewart (1975) model have been widely used. In the model, the parameter of the remaining fraction of the water-drop mass is variable and decisive (eq 8), and can be calculated by the law of conservation of mass (hereafter, the remaining fraction of raindrop mass calculated by this method is denoted as $F_{raindrop}$),~~

$$F_{raindrop} = \frac{m_{end}}{m_{end}+m_{ev}} \quad \text{(eq8)}$$

~~Here, the mass of the reaching ground raindrop after evaporation is m_{end} and the evaporated raindrop mass is m_{ev}. The parameter of m_{ev} is composed of the evaporation rate and fall time of the drop. Kinzer and Gunn (1951) and Best (1950a) have parameterized these two variables, respectively. For the detailed calculation processes, please refer to the supplemental material (Appendix B), or Wang et al. (2016b), Sun et al. (2020), Kong et al. (2013), and Salamalikis (2016).~~

~~Due to the intrinsic limitations of Stewart's model, which is a mixing model between the starting and the final isotopic composition, it assumes a homogenous sub-cloud layer in terms of temperature and humidity (Salamalikis et al., 2016). Here, considering the location of our study site, we reasonably assume that precipitation forms close to the average cloud base at about the 850 hPa (~1500 m) isobaric level (Kong et al., 2013; Li et al., 2016a; Salamalikis et al., 2016). The cloud base temperature and RH were obtained from the moist adiabatic ascent of an air parcel from the surface with initially measured temperature and RH (Appendix A). It is worth noting that the results~~

~~may be affected by errors originating from assumed cloud base heights and calculated vertical profiles of temperature and RH. In the future, the pieces of evidence from direct measurement of cloud base heights, temperature, and RH from radiosondes or aircraft will validate the assumed below-cloud profiles presented here.~~

~~Now, with the emergence of a laser-based spectrometer, high-precision, high-resolution water vapor isotopic composition measurement is becoming easier, and thus the evaluation of below-cloud evaporation is becoming more direct. However, little work has systematically evaluated the differences of F_t computed by different methods. Here, we respectively used the isotope and mass conservation methods to calculate the F_t, and compared their differences.~~

2.5.4 Statistical Analysis

To compare the difference of the below-cloud evaporation calculated by the two methods, the independent t-test was performed on SPSS 13.0 (SPSS Inc., Chicago, US). A significant statistical difference was set at $p < 0.05$.

3 Results and discussion

3.1 Relationship between water vapor and precipitation isotopic ~~ratios~~compositions

Influenced by the below-cloud evaporation, the slope of the local meteoric water line (LMWL) would be lower than 8, the precipitation isotopic composition become more positive, the d-excess of precipitation would be less than 10, and the equilibrium calculated water vapor isotopic composition would be more positive than the observed one. As shown in Figure 2, the LMWL is: $\delta^2H_p=7.0\times\delta^{18}O_p+3.0$ based on event precipitation isotopic composition, and the local water vapor line (LWVL) is: $\delta^2H_v=7.~~6~~8\times\delta^{18}O_v+~~10.0~~15.1$ based on ~~daily~~ per-event water vapor isotopic composition. Both the slope and intercept of LMWL are lower than the Global Meteoric Water Line (GMWL) which are 8.0 and 10.0 (Dansgaard, 1964; Gat, 1996), respectively, indicating the potentially significant below-cloud evaporation effect ~~of below-cloud evaporation~~ on precipitation (Froehlich et al., 2008). In general, the slopes of the meteoric water lines are indicative of kinetic processes superimposed on the equilibrium fractionation, and the little lower slope of LWVL (slope=7.~~6~~8) than the expected equilibrium fractionation (slope=8.0) may also relate to the increasing influence of kinetic

processes (Rangarajan et al., 2017).

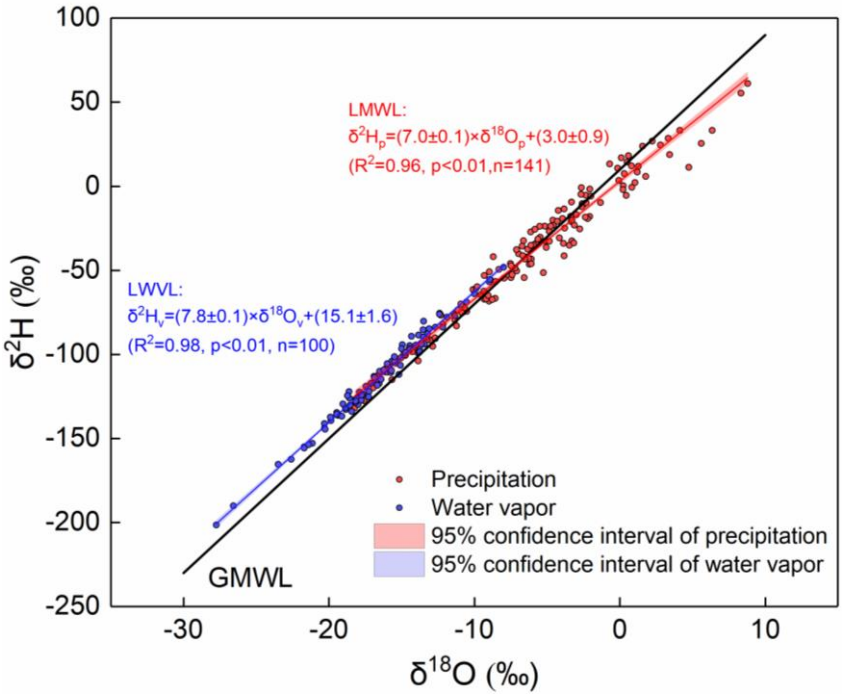

Figure 2 Local meteoric water line (LMWL) and Local water vapor line (LMVL) in Xi'an.

Besides, we note that the water vapor and precipitation isotopic composition basically distribute in different range~~s~~ values, which the former ~~and the water vapor isotopic composition~~ is generally more negative than the ~~precipitation isotopic composition~~latter (Fig. 2). According to the classical isotopic fractionation theory, the heavier isotopes preferentially condense into the liquid phase during the precipitation process, which ~~resulting~~ results in the precipitation isotopic ~~ratios~~ composition more positive than the ~~corresponding~~ water vapor one ~~during the precipitation process~~ (Dansgaard, 1964). Hence, the ~~perfect~~ distribution characteristics of water vapor and precipitation on the $\delta^{18}O$-δ^2H plot would make us suppose that ~~the precipitation and water vapor isotopic composition~~their isotopic compositions are in or close to equilibrium in this study site. To validate our assumption, we plot ~~the relationship between the per-event precipitation and the corresponding day's water vapor isotopic compositions~~their relationship in ~~Figure~~ Fig. 3a~~,~~ ~~as~~ As expected, they show a significant positive correlation (R^2=0.~~66~~70, p<0.01). The water vapor isotopic composition can explain ~~above 60~~70% of the variation of precipitation isotopic composition. Further, we use the measured precipitation isotopic composition to deduce the water vapor isotopic composition at the ~~cloud base~~ground level ~~(1500m)~~ according to the liquid-vapor equilibrium isotope fractionation, and compare ~~it with the observed near-ground water vapor isotopic composition~~them in Fig. 3b. As expected, the scatterplot of the observed

$\delta^{18}O_v$ against the deduced $\delta^{18}O_{pv\text{-}eq}$~~eq(1500m)~~ also presents a significantly positive relationship~~, and the correlation coefficient increases by 4%~~ (Fig. 3b).

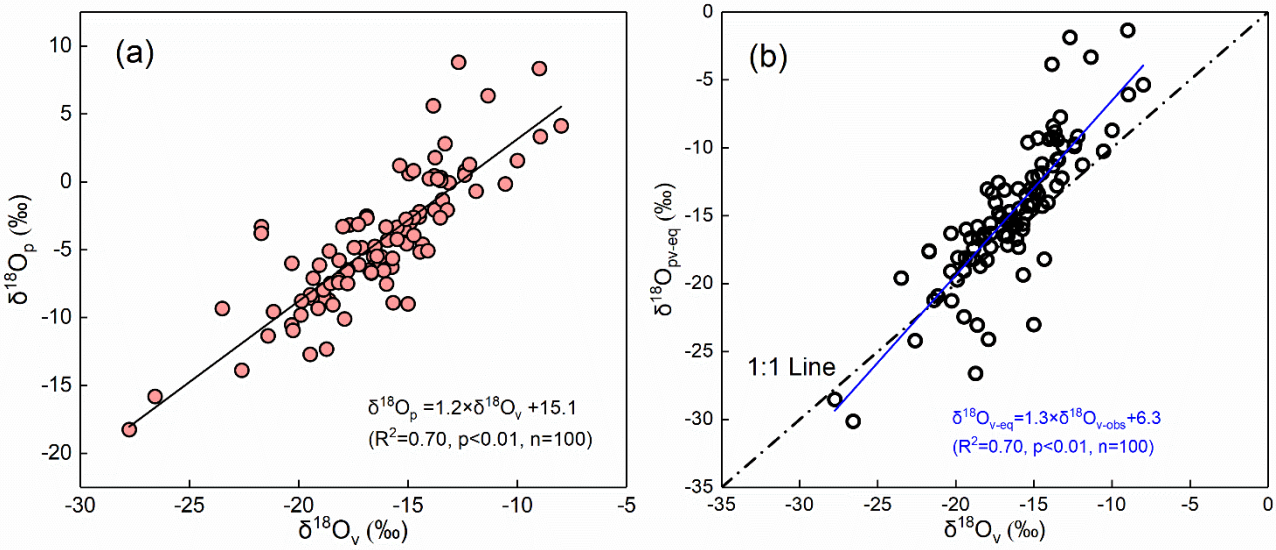

Figure 3 Relationship between $\delta^{18}O_p$ of precipitation and $\delta^{18}O_v$ of water vapor in Xian (a); and relationship between the equilibrium computed ~~1500m~~ $\delta^{18}O_{pv\text{-}eq}$ based on the precipitation isotopic composition and the near ground observed $\delta^{18}O_v$ (b). The dash-dot line in (b) stands for the 1:1 line, and the blue line represents the regression line of the data.

In addition, we also noted that the equilibrium $\delta^{18}O_{pv\text{-}eq}$ is relatively more positive than the observed $\delta^{18}O_v$ (Fig. 3b). Due to the Xi'an city belonging to the semi-arid area, the raindrop is likely to be evaporated in the unsaturated environment during its falling. Therefore, the positively $\delta^{18}O_{pv\text{-}eq}$ is caused by the non-equilibrium fractionation in low relative humidity, which makes the $\delta^{18}O_{pv\text{-}eq}$-$\delta^{18}O_v$ points deviation from the 1:1 line.

The reasonable agreement of ~~$\delta^{18}O$ between~~ observed ~~water vapor~~ and equilibrium ~~prediction~~ water vapor isotopic composition has been reported by Jacob and Sonntag (1991), Welp et al. (2008), and Wen et al. (2010), however, they postulated the different relationships underlying the $\delta^{18}O_v$ and $\delta^{18}O_{pv\text{-}eq}$. Jacob and Sonntag (1991) suggested that the water vapor isotopic composition is possible to be deduced from the corresponding precipitation isotopic composition, but Wen et al. (2010) speculated that the equilibrium method cannot accurately predict the ground-level water vapor isotopic composition in arid and semiarid climates because of two monthly equilibrated water vapor ~~precipitation~~ values deviating the observed ~~water vapor~~ values. Here, with two-year continuous observation, the mean difference between the $\delta^{18}O_{v\text{-}obs}$ and $\delta^{18}O_{pv\text{-}eq}$~~(1500m)~~ is −1.1‰ for $\delta^{18}O$, -8.1‰ for δ^2H, and 0.7‰ for d-excess. Although there is a good relationship between $\delta^{18}O_v$ and $\delta^{18}O_{pv\text{-}eq}$ in our data, the below-cloud evaporation has significant influence on the precipitation isotopic composition,

especially in the arid area. Therefore, it should be cautious to derive the water vapor isotopic composition from the precipitation one., and our results indicate that it is possible to derive the isotope composition of atmospheric water vapor based on that of the precipitation in the semi-arid area. It is worth noting that we do not propose to extract the water vapor isotope time series from precipitation data. Because, in dry regions of the world, precipitation events are rare so deriving vapor isotopes from precipitation can be very misleading. No data is available for the sometimes long dry spells without precipitation. These periods are likely to exhibit very special vapor isotope signals about which no information can be gained from precipitation data.

In addition, we also noted that the equilibrium calculated $\delta^{18}O_{v\text{-}eq(1500m)}$ is relatively more positive than the $\delta^{18}O_{v\text{-}obs}$ (Fig. 3b). In theory, the water vapor isotopic composition decreases with altitude (Deshpande et al., 2010; Salmon et al., 2019). However, due to the CLP belonging to the semi-arid area, the raindrops are likely to experience evaporation in the unsaturated. Therefore, the positively equilibrated $\delta^{18}O_{v\text{-}eq(1500m)}$ is caused by the kinetic fractionation in low relative humidity, and this also makes the $\delta^{18}O_{v\text{-}eq}$-$\delta^{18}O_{v\text{-}obs}$ points deviate from the 1:1 line.

3.2 Below-cloud processes indicated by ΔdΔδ-diagram

Traditionally, to qualitatively assess the below-cloud evaporation of raindrops, the value of d-excess$_p$ is a benchmark, as the isotopically kinetic non-equlibrium fractionation will cause d-excess$_p$ to deviate from 0‰, which is a theoretical value under vapor-liquid equilibrium fractionation at temperatures around 20°C (Gat, 1996). The global mean value of 10‰ for the d-excess$_p$ in precipitation indicates that evaporation is in general a non-equilibrium process. Normally, below-cloud evaporation will move decrease d-excess$_p$ below 10‰, and in comparison, mixing with the recycled water vapor from surface evaporation and plant transpiration will bring increase d-excess$_p$ above 10‰ (Craig, 1961; Dansgaard, 1964). Kinetic (nNon-equilibrium fractionation) is due to the differences in diffusivities of the individual water molecules. Therefore, during the moisture transportation, the water vapor d-excess$_v$ may be modified, and this enhances the uncertainty to gauge the below-cloud evaporation process by solely using d-excess$_p$. In contrast, the ΔdΔδ-diagram introduced by Graf et al. (2019) provides richer information on the below-cloud processes.

Theoretically, on the ΔdΔδ-diagram, Δd<0‰ and Δδ>0‰ indicate the below-cloud

evaporation process, Δδ<0‰ represent that the falling raindrop is less influenced by below-cloud evaporation and retains the cloud signals, and Δd and Δδ close to 0‰ suggest equilibrium conditions. By projecting our data on the ΔdΔδ-diagram~~ΔdΔδ plot~~, the evaporation, equilibration, and non-exchange (e.g., a snowfall event, or a transition from rain to snow with a stronger cloud signal) processes could be clearly differentiated (Fig. 4). It is apparent from Fig. 4, that most of the ~~precipitation~~ rainfall samples are located in the fourth quadrant with positive $\Delta\delta^2H_v$ and negative $\Delta d\text{-excess}_v$, indicating that evaporation is the ~~dominant~~major below-cloud process. ~~A small part of the samples is distributed in the first and second quadrant, and their Δδ are close to 0‰ while Δd are a little higher than 0‰. This cluster of samples implies that the below-cloud evaporation and cloud-based isotopic fractionation tend to achieve a complete equilibrium state.~~ Interestingly, ~~in our samples,~~ most of the snowfall samples seize the second and third quadrant with negative $\Delta\delta^2H_v$, which is suggestive of below-cloud evaporation with less impact on them, and their initial signal is well retained after the cloud-based equilibrium fractionation~~ is well retained~~.

According to the results ~~from~~ of numerical simulations and in-situ observations, Graf et al. (2019) summarized that raindrop size and precipitation intensity appear to be the important driving factors of the below-cloud processes, because raindrops with large diameter and ~~high~~ heavy precipitation intensity will reduce their residence time in the atmospheric column, and lower the evaporation possibility during its way down toward the ground surface. However, as for snowfall events, it seems unreasonable to explain the strongly negative $\Delta\delta^2H_v$ ~~from through~~by the raindrop size and rain rate (Fig. 4). It is well known that snowfall events generally happen in low-temperature conditions, and correspond to weak evaporation, ~~due to~~in addition, the ~~lower~~ diffusion speed of the ice phase (solid) to vapor is lower than ~~as compared to~~that of liquid to vapor. Hence, rain/snow formed under such circumstances, ~~its~~ the isotopic signals will be ~~not be largely changed~~less impacted by the environmental factors during its falling~~, . which~~ This leads the Δδ to be more negative with the decrease of temperature, such as the phenomenon observed in Graf's et al. (2019) study during the post-frontal periods. Our results suggest that in addition to raindrop size and rain rate, precipitation type is also an essential factor ~~that needs to~~should be fully considered in the below-cloud

processes.

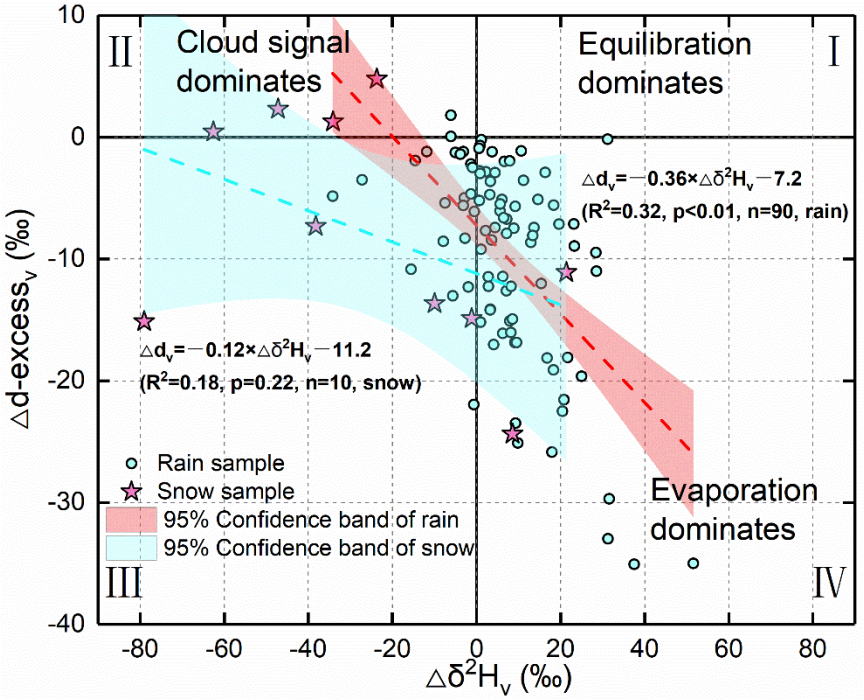

Figure 4 The projection of our data on the suggested ΔdΔδ-diagram by Graf et al. (2019) ~~suggested ΔdΔδ-diagram~~. The solid lines stand for Δd-excess$_v$ and $\Delta\delta^2H_v$ of 0‰. The dashed line corresponds to the linear fit through the samples with the 95% confidence band in ~~red~~ shading. The red line is for rainfall samples, and the cyan line is for snowfall samples. The upper Roman represent the category of quadrant.

The slope of ~~the regression line of~~ Δd/Δδ ~~Δd/Δδ~~ is -0.~~15~~36 for rainfall samples and -0.12 for snowfall samples in our study (Fig. 4). In Graf's et al. (2019) study, they reported a Δd/Δδ slope of -0.3. It should be noted that the slope of Graf's et al. (2019) is based on intra-event samples, while ours is on per-event samples. Although the time scales are different in the two studies, interestingly, the rainfall slopes are close to each other, and the snowfall slope is obviously different with rainfall slope. The Δd/Δδ slope of -0.3 could represent a general characteristic of rainfall for continental mid-latitude cold front passages (Graf et al., 2019). Xi'an city is located near the 35°N in inland of China, which just belongs to the scope of continental mid-latitude. In comparision, the Δd/Δδ slope of our snow samples is less negative. Therefore, the different Δd/Δδ slopes might be related to the different climatic characteristics or precipitation types. Certainly, to validate this assumption, more works need to be done in future studies.

~~, which is half of the slope shown by Graf's et al. (2019). However, the slope of Graf's et al. (2019) is based on intra-event samples, while ours is on per-event samples, hence the two slopes cannot compare with each other directly.~~

~~To advance the understanding of the slope, the controlling factors have been analyzed.~~

According to the sensitivity test by Graf et al. (2019), RH has a considerable impact on the slope of Δd/Δδ. Low RH is coupled with more negative slopes, while the slopes of Δd/Δδ under high RH conditions are less negative or even positive (Fig. 5c). In addition, the temperature has a similar impact on the slopes of Δd/Δδ as the RH (Fig. 5a). This indicates that the negative slopes of Δd/Δδ correspond to a warm and dry environment. Besides, the slopes of Δd/Δδ may relate to the precipitation types. When the samples are separated into rainfall and snowfall, the rainfall slope is -0.28 and the snowfall slope is only -0.12. Although the time scales are different in the two studies, interestingly, the slopes of rainfall are more close to each other. The slope of -0.3 could represent a general characteristic of rainfall for continental mid-latitude cold front passages (Graf et al., 2019), while the slope of snow samples is less negative in our study (Fig. S3).

Meteorological factors, such as precipitation amount, temperature, and RH, are the main factors affecting below-cloud evaporation (Li et al., 2016b; Peng et al., 2007), and have been well studied by combined with precipitation d-excess$_p$ (Ma et al., 2014; Wang et al., 2016b). In order to further analyze the below-cloud processes, we add the meteorological and isotopic information on the ΔdΔδ-diagram (Fig. 5). Generally, with regard to high Δ^2H_v samples, the corresponding meteorological condition is high temperature, low precipitation amount, and low RH (Fig. 5a-c). In contrast, under a condition of low air temperature, high RH, and large precipitation amount, the Δ^2H_v of samples are relatively more negative (Fig. 5a-c). As below-cloud processes are controlled by multi-variable factors, it is hard to only use single physical variable to explain the below-cloud evaporation (Ma et al., 2014; Wang et al., 2016b). For example, under the highest temperature condition (two most red dots in Fig. 5a), the below-cloud evaporation effect should be higher, and cause Δ^2H_v to be more positive and Δd-excess$_v$ to be more negative. However, under such circumstances, both the Δ^2H_v and Δd-excess$_v$ of the two samples are close to 0‰. By considering the precipitation amount, the two samples collected under the highest temperature condition are associated with a relatively larger precipitation amount which will temper the intensity of below-cloud evaporation. In addition, higher temperature corresponds to higher saturation vapor pressure, and a larger number of water molecules present in the atmosphere, which may enable substantial, rapid equilibration of water molecules between raindrops and ambient vapor during fall. Similarly, the samples with lower precipitation amount are associated with high RH, and cause the Δ^2H distributed

around 0‰. For the snow samples, the data with positive Δ^2H is related to the very

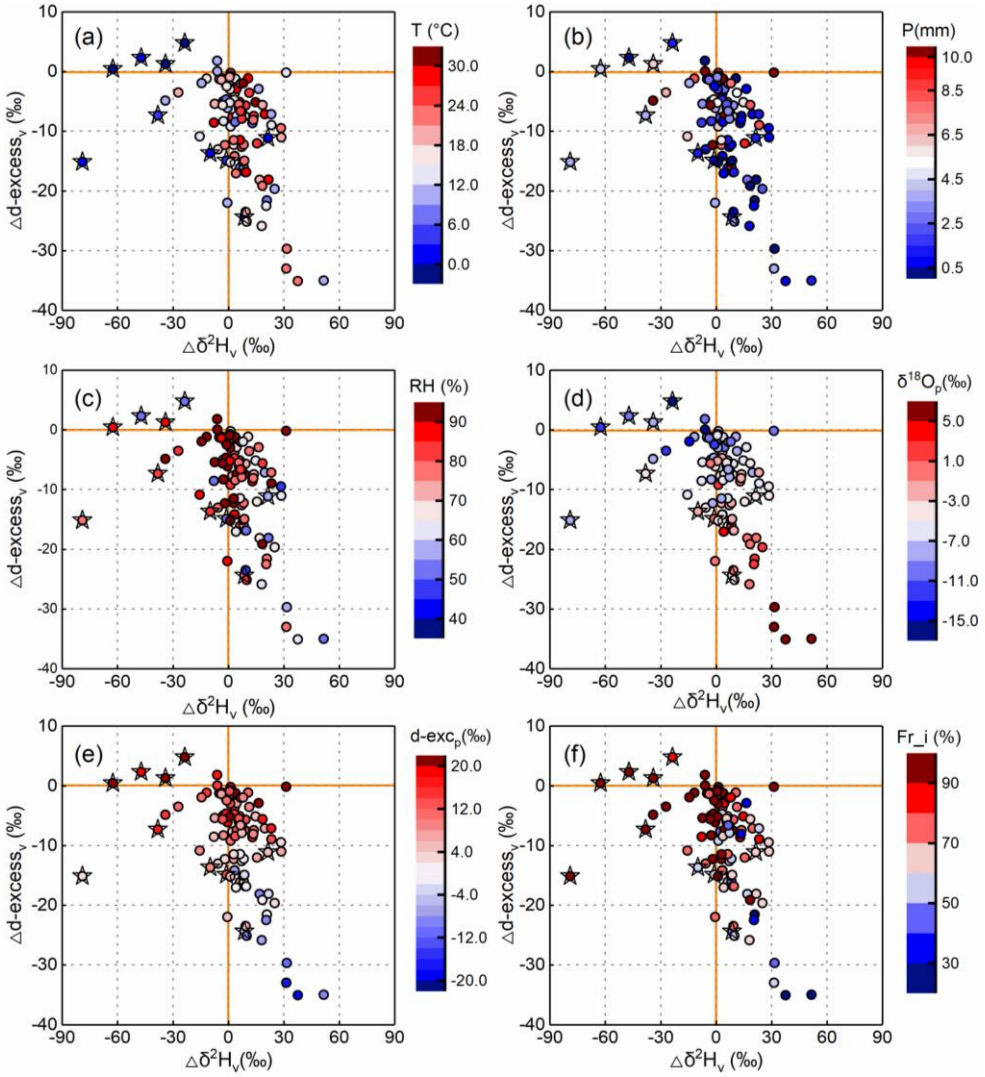

low RH (Fig. 5c).

Figure 5 ΔdΔδ-diagram for the precipitation samples with meteorological factors and precipitation isotopic information. Temperature (a); Precipitation amount (b); Relative humidity (c); $\delta^{18}O_p$ of precipitation (d); d-excess$_p$ of precipitation (e); Remaining fraction of evaporation (f). The dots with a star represent the snow samples.

In contrast to meteorological factors, the pattern of precipitation isotopic composition distribution on the ΔdΔδ-diagram is more clear. Under the high below-cloud evaporation condition, the $\delta^{18}O_p$ is more positive and d-excess$_p$ is relatively negative (Fig. 5d and 5e). Correspondingly, the differences between equilibrated $\delta^2H_{eq\text{-}v}$, d-excess$_{eq\text{-}v}$ and observed $\delta^2H_{gr\text{-}v}$, d-excess$_{gr\text{-}v}$ are larger. Conversely, under low below-cloud evaporation conditions, mainly corresponding to the most snow samples, we could see the lowest $\delta^{18}O_p$ and highest d-excess$_p$ samples, respectively (Fig. 5d and 5e). Moreover, the Δ^2H_v is lower than 0‰ and Δd-excess$_v$ is placed around 0‰. Basically, the ΔdΔδ-diagram follows not only the traditional explanation that Δd<0‰

~~and Δδ>0‰ indicate the below-cloud evaporation process but also provides more information on the falling raindrops, such as Δd<0‰ and Δδ<0‰ indicating the cloud signals, and Δd and Δδ close to 0‰ indicating equilibrium conditions.~~

~~The slope of the regression line of Δd/Δδ is ~0.15 in our study (Fig. 4), which is half of the slope shown by Graf's et al. (2019). However, the slope of Graf's et al. (2019) is based on intra-event samples, while ours is on per-event samples, hence the two slopes cannot compare with each other directly. To advance the understanding of the slope, the controlling factors have been analyzed.~~

~~According to the sensitivity test by Graf et al. (2019), RH has a considerable impact on the slope of Δd/Δδ. Low RH is coupled with more negative slopes, while the slopes of Δd/Δδ under high RH conditions are less negative or even positive (Fig. 5c). In addition, the temperature has a similar impact on the slopes of Δd/Δδ as the RH (Fig. 5a). This indicates that the negative slopes of Δd/Δδ correspond to a warm and dry environment. Besides, the slopes of Δd/Δδ may relate to the precipitation types. When the samples are separated into rainfall and snowfall, the rainfall slope is ~0.28 and the snowfall slope is only ~0.12. Although the time scales are different in the two studies, interestingly, the slopes of rainfall are more close to each other. The slope of ~0.3 could represent a general characteristic of rainfall for continental mid-latitude cold front passages (Graf et al., 2019), while the slope of snow samples is less negative in our study (Fig. S3).~~

~~Certainly, to explore the relationship between the slope of Δd/Δδ and the climatic characteristics and precipitation types, more validation works need to do in future studies.~~

3.3 Comparing and analyzing the <u>two Methods</u>~~differences between F_{iso} and $F_{raindrop}$~~

3.3.1 ~~The differences and reasons~~<u>Quantitatively evaluated the below-cloud evaporation effect by the two methods</u>

<u>The ΔdΔδ-diagram provide the rich information on the below-cloud processes, but it is only a qualitative analysis. In comparison, the quantitative evaluation is more important to indentify the below-cloud evaporation effect on the precipitation isotopic composition. Here, we chose two methods to respectively calculate the variations of $\Delta\delta^2H_p$ and evaporation fraction (F_i) on per-event precipitation, and compared their differences.</u>

The $\Delta\delta^2H_p$ range from 0 to 131.1 ‰ with an average and standard deviation of 17.8 ± 23.8 ‰, and the F_i range from 0 to 82.7 % with an average and standard deviation of 16.3 ± 21.9 % (n=141) for the method 1. The $\Delta\delta^2H_p$ range from -73.8 to 82.5 ‰ with an average and standard deviation of 16.3 ± 24.4‰, and the F_i range from 0 to 67.6 % with an average and standard deviation of 22.1 ± 21.7 % (n=100) for the method 2. For the 100 precipitation events with corresponding water vapor data, the averages and standard deviations are 20.8 ± 25.5 ‰ for $\Delta\delta^2H_p$ and 22.0 ± 22.4 % for F_i computed by the method 1. According to the independent t-test, there are no statistic differences on the $\Delta\delta^2H_p$ ($F=0.016$, $p=0.20$, $n=100$) and F_i ($F=0.086$, $p=0.97$, $n=100$) for the two methods.

As shown in Fig. 5a and Fig. 5b, the $\Delta\delta^2H_p$ and F_i in the two methods have similar fluctuation trend. The positive $\Delta\delta^2H_p$ and high F_i are appeared from March to July, while the negative $\Delta\delta^2H_p$ and low F_i are shown from September to February. In addition, the most positive $\Delta\delta^2H_p$ values are captured by method 1, while the most negative values are detected by method 2. In order to analyze the underlying reason, we checked the equation used to calculate $\Delta\delta^2H_p$. We noted that in eq 6 the F_r is always lower than 1, and thus (F_r^{β}-1) is negative. Similarly, the $\frac{\gamma}{\alpha}$ is smaller than 1, and thus ($1-\frac{\gamma}{\alpha}$) is also negative. Therefore, the $\Delta\delta^2H_p$ calculated by the method 1 could not be a negative. In the method 2, the most negative $\Delta\delta^2H_p$ values are related to the snowfall events. During the supersaturation process, vapor deposition occurs over ice (Jouzel and Merlivat, 1984), which causes the snow isotopic composition at ground-level to be more depleted than its formation height. In fact, the mass of the snow also increase in the supersaturation condition, however, the method 1 only considers the evaporation process. The diameter of raindrop used to determine the terminal velocity of the raindrop and the evaporation intensity (Supplemental material, eq 9) do not account for snowfall factor which results in a great uncertainty in the calculation. Therefore, the method 1 is not suit for evaluating the below-cloud effects on the precipitation isotopic compostion when the snowfall or low temperature rainfall events.

In addition, the influence of below-cloud evaporation effect on the δ^2H_p is heavier in method 1 than in method 2, especially at higher F_i conditions (Fig. 5c), because the slope of $F_i/\Delta\delta^2H$ in method 1 (1.00 ‰/%) is a little steeper than in method 2 (0.91 ‰/%), and the intercept in method 1 (-1.65) is gentler than in method 2 (-3.97). Thus, under the same evaporation intensity, the $\Delta\delta^2H_p$ is more enriched in method 1 than in method

2.

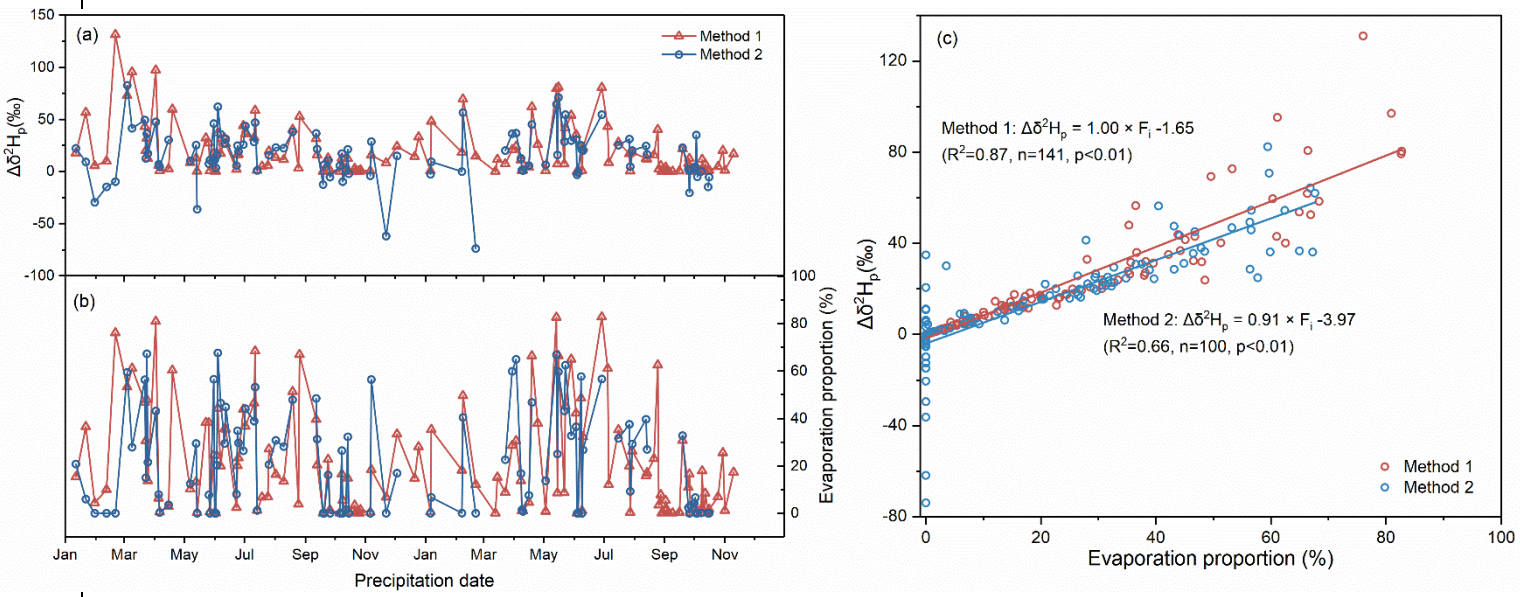

On ~~a~~ the seasonal scale, both methods show that the below-cloud evaporation effect is heavier in spring and summer and weaker in autumn and winter (Fig. SXX). Their differences are smallest in spring and largest in winter. The significant difference in winter might be related to the supersaturation process.

~~the difference between F_{iso} and $F_{raindrop}$ in spring, summer, autumn, winter is 13.7%, 12.8%, 6.0%, and 25.0%, respectively, which is the largest in winter, and the lowest in autumn (Fig. 7).~~ Figure ~~7~~6 Comparison between the mean remaining fraction results calculated by two methods in four seasons. n represent the number of samples used in statistics.

~~In 1975, Stewart (1975) presented a set of empirical models, which is still widely used, to evaluate the below-cloud evaporation rate of the falling raindrop. However, Limited by measuring the cloud-based isotopic composition of the raindrop, many studies turn to use mass conservation model to evaluate the evaporation rate of the raindrop during its falling (Kong et al., 2013; Li et al., 2016a; Sun et al., 2020; Wang et al., 2016b). Here, for comparing their differences, we used the isotope method and mass conservation model to calculate the F_i after the below-cloud evaporation, respectively. For both methods, we only considered evaporative exchange in below-unsaturation cases. However, it is not true for the isotopic method, because both the evaporation and equilibration have effects on the Δδ of the droplet during its falling from the cloud base.~~ Here, it should be noted that in method 2 we assume that the below-cloud precipitation and surrounding ambient water vapor are in fully isotopic equilibrium, and F_i only accounts for the evaporation effect on Δδ and is overlooked the equilibrium

fractionation. Therefore, the $\Delta\delta F_{iso}$ results may ~~underestimate~~overestimate the ~~remaining fraction of evaporation~~below-cloud evaporation effect. To get the accurate F_{iso} results, more works need to ~~do to~~ partition the equilibration process from the evaporation in the future.

~~we assumed that the below-cloud precipitation and surrounding ambient water vapor are in fully isotopic equilibrium, and F_{iso} only accounts for the evaporation effect on Δδ. Therefore, the F_{iso} results may underestimate the remaining fraction of evaporation. To get the accurate F_{iso} results, more works need to do to partition the equilibration process from the evaporation in the future.~~

~~As shown in Fig. 6a, the computed mean of reaming fraction is 76.3% by the isotopic method (F_{iso}), and 65.6% by the mass conservation model ($F_{raindrop}$) based on two-year statistical results. The $F_{raindrop}$ is statistically lower than the F_{iso} depending on the independent t-test (F=1.49, p<0.01). In addition, the F_{iso} and $F_{raindrop}$ show an obvious difference, and that is the F_{iso} and $F_{raindrop}$ seriously deviating from 1:1 line, when the F_{iso} equals to 60%~80% (Fig. 6b). On a seasonal scale, the difference between F_{iso} and $F_{raindrop}$ in spring, summer, autumn, winter is 13.7%, 12.8%, 6.0%, and 25.0%, respectively, which is the largest in winter, and the lowest in autumn (Fig. 7).~~

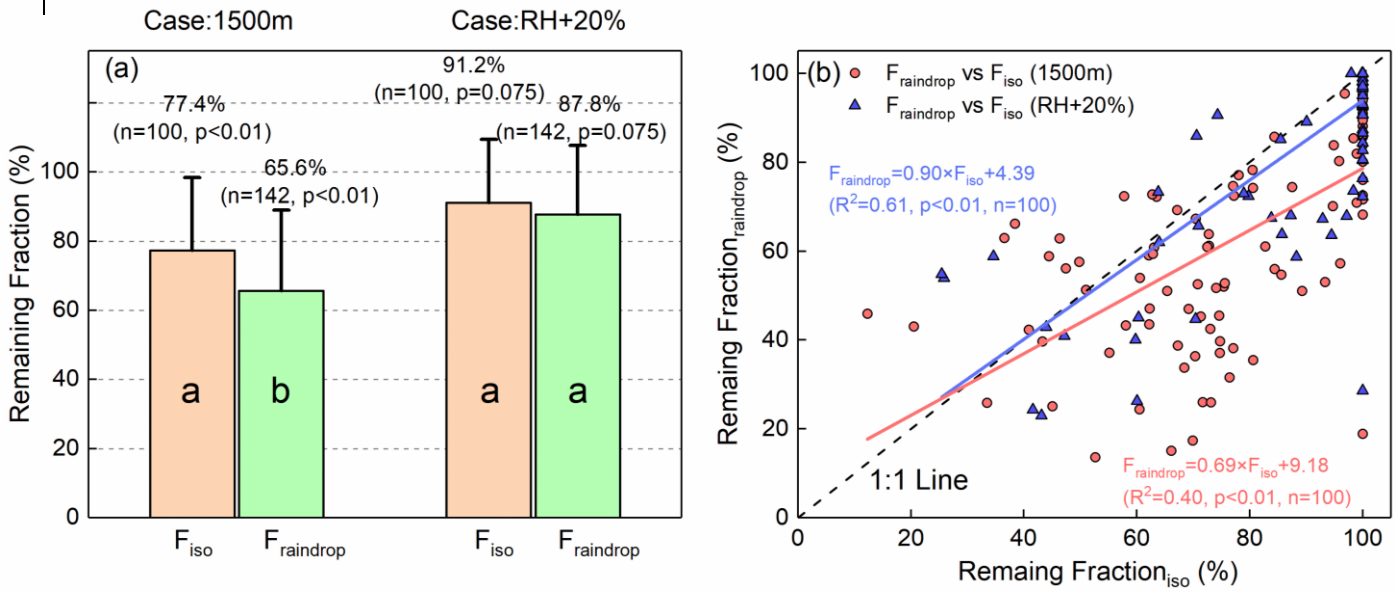

~~Figure 6 The comparison between the remaining fraction calculated by two methods. In (a), the taupe bars and the abbreviation of F_{iso} represent the remaining fraction calculated by the isotopic method, and the green bars and the abbreviation of $F_{raindrop}$ represent the remaining fraction calculated by the mass conservation method. Case 1500m denotes that the raindrops evaporation calculation is based on the assumption of the cloud base at 1500m, and the raindrops are formed at that altitude. Case RH+20% denotes that based on the condition of case 1500m, we calculated the remaining fraction by increasing the ground observed RH by 20%. n represents the number of samples used in statistics. The a and b in the bars denote the results of the independent t-test. In (b), the red dots represent the computed results of the~~

~~remaining fraction under case 1500m condition, and the blue triangles represent the computed results under case RH+20% condition. The dash line is the 1:1 line.~~

3.3.2 Meteorological controls on the two methods

To further explore the ~~reason for the large~~ differences by employing the ~~different~~two methods, we performed the correlation analyses between meteorological factors and the $\Delta\delta^2H_p$~~remaining fraction of evaporation~~ (Fig. ~~S4~~6). These analyses reveal that the most important impact factor ~~both~~ on ~~F_{iso} and $F_{raindrop}$~~both methods is RH (Fig. ~~S4b~~6b). Although precipitation amounts have influences on ~~F_{iso} and $F_{raindrop}$~~both methods as well, their relationships are non-linear or~~, and~~ its effect on $\Delta\delta^2H_p$~~F_{iso}~~ is rather weak (~~r~~R^2=~~0.16~~0.49, method 1; r=-0.30, method2; Fig. ~~S4c~~6c). For temperature, no clear correlation was found for method 1 (r=0.05), and the positive correlation is weak for method 2 (r=0.42). Wang et al. (2016b) explicitly pointed out that among the parameters of temperature, precipitation amount, RH, and raindrop diameter, RH generally plays a decisive role on the ~~obtained~~ Δd-excess~~, which is positively correlated with the remaining fraction of raindrop~~.

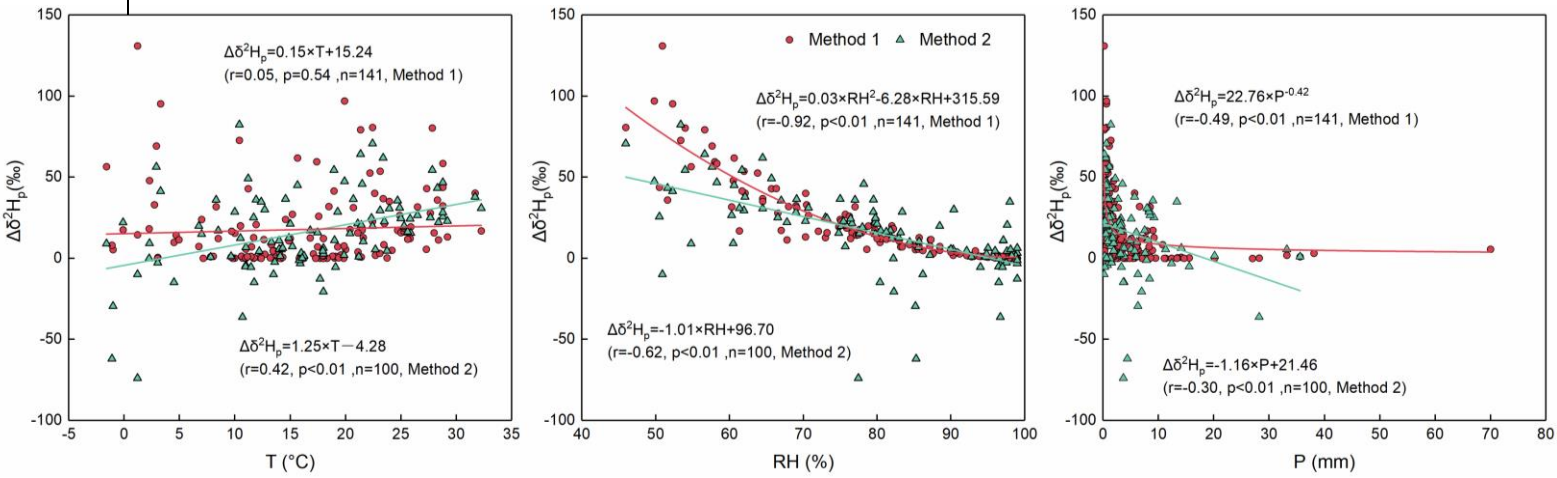

~~Figure 7 Comparison between the mean remaining fraction results calculated by two methods in four seasons. n represent the number of samples used in statistics.~~

In both methods, in an arid environment with high temperature, low relative humidity, and small precipitation amount the evaporation effect on the $\Delta\delta^2H_p$ is large. However, in the low temperature conditions (below 5 °C), there is a divergence on $\Delta\delta^2H_p$ for the two methods, which is partly attribute to the supersaturation condition. With increasing relative humidity, $\Delta\delta^2H_p$ becomes closer to 0, but the variation of $\Delta\delta^2H_p$ is large for method 2 and very limited for method 1 when the relative humidity is higher than 80%. There is a wide range, from 0 to 130 ‰, for $\Delta\delta^2H_p$ when the precipitation amount is small. As the precipitation amount is above 10 mm, the value of $\Delta\delta^2H_p$ tends toward 0 ‰.

~~In order to analyze the underlying reason, first, we checked the equation used to calculate F_{iso} and $F_{raindrop}$. We noted that in both methods, RH is an important parameter to compute the remaining ratio. In the equation for computing F_{iso}, the values of γ and β are highly dependent on RH. Equally, in the $F_{raindrop}$ computing equation, RH will be the decisive factor of evaporation intensity (E). Then, we tested the sensitivity between $\Delta\delta^{18}O$ and RH under different F_{iso} levels (Fig. S5). Our results showed, under high RH condition (60%~90%), a little variation of $\Delta\delta^{18}O$ corresponded to a wide range of F_{iso} distribution. We also noticed, under higher RH condition (above 90%), the simulated $\Delta\delta^{18}O$ is very small, normally lower than 0.5‰. However, in reality, the $\Delta\delta^{18}O$ is generally greater than 0.5‰. Therefore, when the actual $\Delta\delta^{18}O$ value is larger than the theoretical value, the calculated F_{iso} results will be larger than 100%, and this is in accordance with the actual condition. Because under higher RH condition, the raindrop evaporation ratio will decrease, and in turn the F_r will appropriately increase. Moreover, in the near-saturated air column, the raindrop is hardly evaporated.~~

~~Therefore, it is reasonable to assume that when the RH is higher, the difference between the F_{iso} and $F_{raindrop}$ will be reduced. To validate our assumption, we computed the F_{iso} and $F_{raindrop}$ by increasing RH by 20%, respectively. As expected, the mean annual difference was highly reduced, and statistically there is no significant difference (Fig. 6a, independent t-test, F=5.665, p=0.075). Moreover, the F_r computed by those two methods is closer to each other, while the correlation coefficient is highly increased, and the slope is closer to 1 (Fig. 6b). For the seasonal variations of F_r, the larger differences between F_{iso} and $F_{raindrop}$ in spring and summer are regarding to the low RH in these seasons, while the small difference in autumn is related to the higher RH. For the largest difference in winter, it is most likely due to the fact that in the mass conservation model, the diameter of raindrop used to determine the terminal velocity of the raindrop (v_{end}) and the evaporation intensity (E) do not account for snowfall factor resulting a great uncertainty in the calculation results.~~

3.3.2 Sensitivity test

In method 1, the input physical parameters include temperature (RH), relative humidity, precipitation amount, and surface pressure. In method 2, the input physical parameters include temperature, relative humidity, and surface pressure. Therefore, these parameters are considered in the sensitivity test.

For RH test, one case adds 10% on the measured RH, and another case substracts

10% on the measured RH. If the RH values are above 100%, then they are artificially set to 99% to conform to reality. Two temperature scenarios, plus and minus 10 °C based on the actual temperature, are analysed. In the sensitivity test of precipitation amount, considering that the amounts are lower than 0.1 mm in some precipitation events, therefore, the reduction lower limit is set at 0.1 mm, and enhancement upper limit is set at 5 mm. On the basic surface pressure condition, 10 kPa pressure fluctuation is considered for its impact.

As shown in Fig. 7, increasing RH and precipitation, and decreasing temperature have negative impact, that is, the below-cloud evaporation effect on the isotopic compostion will be attenuated. On the contrary, decreasing RH and precipitation, and increasing temperature have positive impact indicating that the below-cloud evaporation effect will be strengthened. The varying of surface pressure has no impact on the $\Delta\delta^2H_p$ for both methods. Moreover, the influencing strength of the physical parameters on the $\Delta\delta^2H_p$ are different in the two methods. For example, in method 1, the increases of temperature basically unchange the evaporation effect on the $\Delta\delta^2H_p$, and the influence of decreasing temperature on mitigating evaporation is limited as well. However, the situation is total different in method 2, where the temperature is a decisive factor. In addition, the influence of RH is over temperature in method 1, but the condition is reversed in method 2. Precpitation amount is also an important factor, as the influence of precipitation on $\Delta\delta^2H_p$ even surpass the RH when it is increased of 5 mm. Because of the limited decrease of precipitation amout, its positive feedback is hard to evaluate.

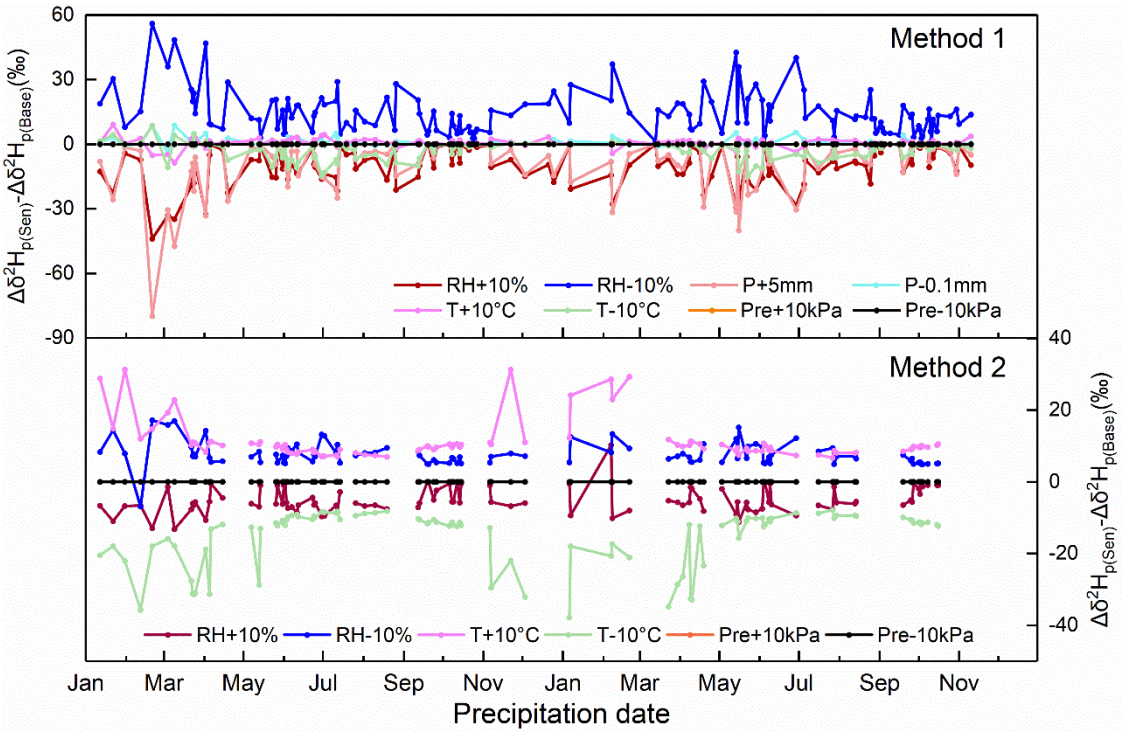

In the calculation of ~~the below-cloud isotopic evaporation model~~method 2 (eq. 8, and supplemental material, eq. XX) ~~(eq. 7)~~, except for the measured groud level precipitation and water vapor isotopic compositions ($\delta_{gr\text{-}p}$ and $\delta_{gr\text{-}v}$), the other two controlling factors are the equilibrium fractionation factor (α) and the ~~RH~~cloud base height. The α is determined by the temperature variations of the cloud base, and cloud base height is related to surface temperature and RH (eq.XX). With RH increase, the cloud base heights decrease, and vice versa (Fig. SXX). In comparison, the cloud base heights are not sensitive to the change of temperature.

~~As the equilibrium fractionation factor varies with the cloud base altitude (mainly caused by the variation of temperature), we used the different altitudes to represent the variations of α. In order to assess the relevance of different ambient conditions for the raindrop evaporation, a sensitivity test of F_r under different altitude and RH scenarios is exhibited in Fig. S6. With the increase of altitude, the F_r is gradually decreased. It is well known that with the increase of altitude, the raindrop falling distance will increase, and correspondingly the falling time will be extended. As a result, more fraction of raindrops would be evaporated in the unsaturated atmospheric columns. When the RH increases by 20%, the atmospheric columns is near saturated, and largely decrease the evaporation possibility of falling raindrops. Conversely, the decrease of RH will strongly increase the evaporation proportion of falling raindrops. In addition, according to Fig. S6, the F_r seems to be more sensitive to the changing of RH than that of altitude.~~

Comparing with the ~~isotopic~~ method 2, ~~there are many parameters in the~~the calculation of ~~mass conservation model~~method 1 is more complex~~,~~. Many variables, such as raindrop diameter, evaporation intensity, raindrop falling velocity, cloud base height, ect., are needed to be considered, while they are convoluted with temperature, RH, precipitation amount, and surface pressure. ~~resulting in the remaining fraction calculated by the mass conservation model with larger uncertainty.~~Through sensitivity test, the RH and precipitation amount are the two decisieve factors in method 1 for deciding the below-cloud evaporation intensity.

~~Taking the F_{iso} results as the benchmark, in our study, the mass conservation method will overestimate the raindrop evaporation ratios. The overestimation may be related to the low RH in our studying location. If we increase the RH by 20%, there is no significant difference between the two methods. This indicates that in high RH areas,~~

~~either method could be used to calculate the F_v. However, in those arid and semi-arid areas, where the RH is relatively low, and the high latitude regions, where snowfall is frequent in winter, we need to cautiously use the result computed by the mass conservation method. Furthermore, Graf et al (2019) emphasized the role of the temperature structure, in particular melting layer height in the influence on the below-cloud processes, that a higher melting layer height prolongs the time for exchange between vapor and rain and leads to stronger equilibration and evaporation. In the future, it is therefore promising to study the raindrop formation heights, temperature profiles (e.g. melting layer heights), and atmospheric water vapor isotopic profiles when considering the below-cloud processes of the raindrops.~~

3.3.2 Uncertainty estimations

There are many uncertainties in the two methods estimates. In method 1, the input parameters include the variation of temperature, RH, precipitation amount, and surface pressure. In method 2, the uncertainty comes from the variations of the input temperature, RH, surface pressure, ground level water vapor $\delta^2H_{gr\text{-}v}$, and precipitation δ^2H_p. However, the variations of surface pressure show no impact on the $\Delta\delta^2H_p$ in the sensitivity test, therefore, it is not considered in the uncertainty calculation.

To check the influence of temperature, RH, precipitation amount, and precipitation δ^2H_p on the below-cloud evaporation effect, we assume that the errors are mainly from the measurement uncertainty of the instrument, which is ± 0.3°C, ± 3%, ± 4% precipitation amount, and ± 1.0 ‰, respectively. Due to the humidity effect (section 2.4), the measured $\delta^2H_{gr\text{-}v}$ for each event has a wide range of uncertainty, which varies from 1.3 to 8.2 ‰. Hence, the lower and upper limits of the above input parameters in method 1 and method 2 are used to quantify the uncertainties and add them quadratically. We obtain the overall uncertainty varying from 0.71 to 0.72‰ for method 1, and from 0.60 to 1.05‰ for method 2 in the estimates of $\Delta\delta^2H_p$ values (refer to supplemental material, appendix XX)

3.4 The characteristics of below-cloud evaporation ~~of raindrop~~effect in Xi'an

~~As~~ Since the ~~phenomenon of~~ below-cloud evaporation is very common in arid and semi-arid regions, it is important to clearly know the variation of precipitation istopic compostion during its falling before ~~to explore~~ exploring the information contained in the precipitation isotop~~ic composition, es.it is important to clearly know that how much~~

~~of the raindrops have been evaporated before they land on the ground.~~ Here, we summarized the seasonal variations of $\Delta\delta^2H$~~F_{iso}~~ in Xi'an by two methods (Fig. 8).

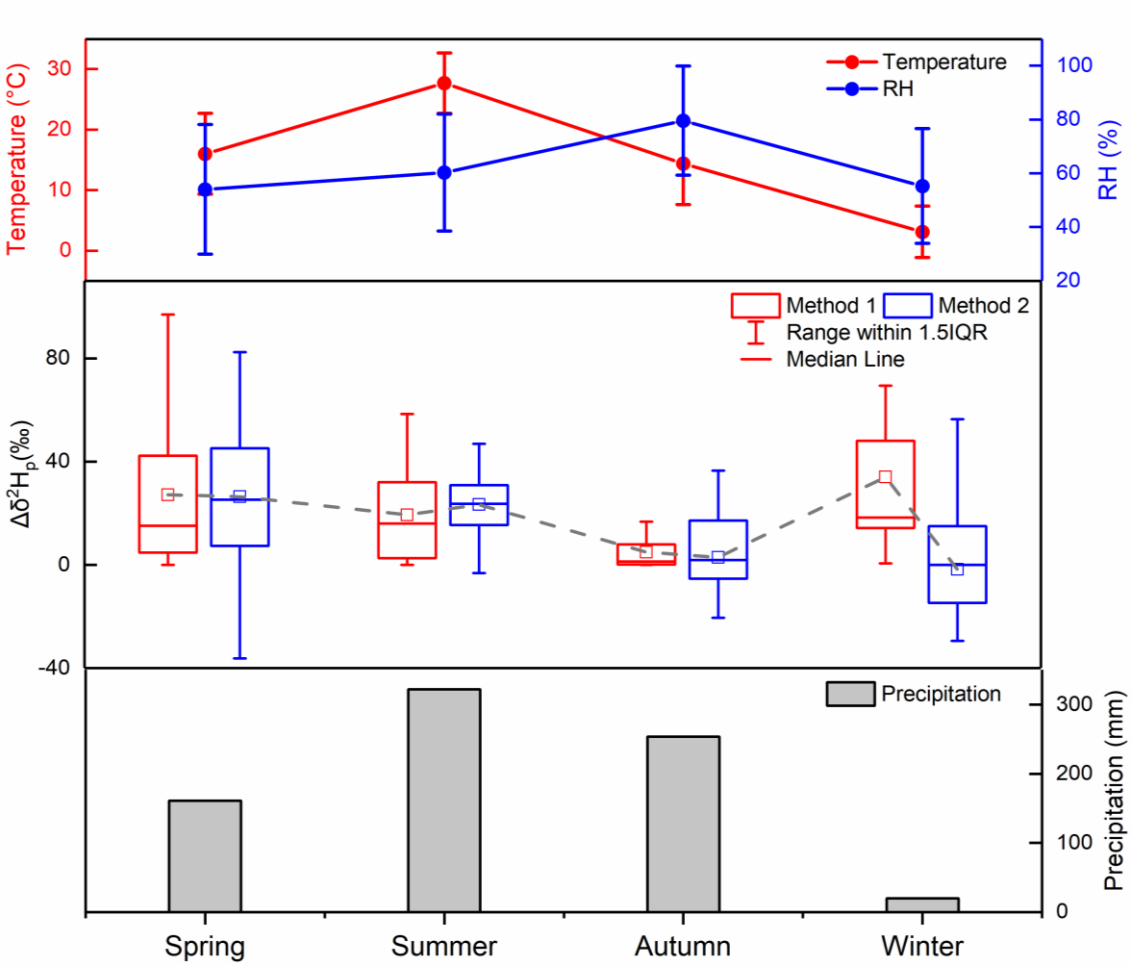

Figure 8 The variations of temperature, relative humidity, precipitation amount and mean remaining fraction of evaporated raindrops in four seasons in Xi'an

By seasonally dividing the precipitation isotopic composition on the ΔdΔδ-diagram, it showed that samples collected in spring and summer dominate the evaporation phase, reflecting a stronger evaporation influence, while most of the winter precipitation and part of autumn precipitation monopolize the cloud signal phase indicating a weak or no below-cloud evaporation, and even supersatuation on these samples (Fig. S7). ~~In addition, part of the autumn samples, of which the below-cloud evaporation and cloud-based isotopic exchange tends to achieve a complete equilibrium state is distributed in the equilibration phase (Fig. S7).~~

Based on quantitativel analysis, ~~The~~ the two methods show similar evaporation effect in spring, summer, and autumn, and different trends in winter. The reason had been

discussed in Section 3.3.1. In addition, the method 1 shows a narrower variation range of $\Delta\delta^2H_p$ than the method 2, because it only considers the below-cloud evaporation process. In method 2, the ~~mean raindrop~~ evaporation effect on δ^2H_p ~~rate~~ is ~~highest~~ powerful in spring and summer, and ~~lowest~~ weaker in autumn and winter based on two-year data (Fig. 8). The seasonal variation of $\Delta\delta^2H_p$~~F_{iso}~~ basically ~~follow~~mirror~~sed~~ the trend of ~~seasonal variation of~~ RH. Although the precipitation amount is highest in the summer, the temperature is extremely high and RH is relatively low, which causes the high ~~evaporation rate~~variation of $\Delta\delta^2H_p$ in summer. In winter, the low $\Delta\delta^2H$~~evaporation rate~~ in method 2 may be related to the precipitation type, because snowfall is the main deposition type in this season.

4 Conclusions

The below-cloud processes of precipitation are complex, variable, and influenced by many factors, especially in the arid and semi-arid regions. Previously, below-cloud evaporation is the most well-studied post-condensation process with the aid of the slope of LMWL and d-excess of precipitation. In comparison, other below-cloud processes, such as the vapor-liquid equilibration, the hydrometeors supersaturation growth ~~between the raindrop and ambient vapor~~, have paid less attention in different rain types. In this study, based on the two-year precipitation data collected in Xi'an, we compiled a set of methods to systematically evaluate the below-cloud evaporation effect on local precipitation isotopic composition~~systematically analyze its below-cloud processes~~, and get the following main conclusions:

1. In arid areas, the precipitation and water vapor isotopic compositions have a good relationship, and therefore the joint observation of the two tracers could provide more information on the precipitation processes. In Xi'an, the below-cloud evaporation effect is stronger in spring and summer, and weaker in autumn and winter, and is related to the variation of local RH.~~In Xi'an, the precipitation isotopic signals mainly record the information of water vapor isotopic composition, but the signals could be changed by the below-cloud evaporation effect. This reminds us to be cautious in using precipitation isotopic compositions to study the hydrological cycle and climate changes in the arid and semi-arid regions.~~

2. Our work validates the general applicability of the ΔdΔδ-diagram. Although there is a difference in timescale between Graf's et al. (2019) study (intra-event) and ours (per-event), ~~by presenting our per-event precipitation isotopic results on the ΔdΔδ-diagram~~, the influence of below-cloud processes ~~and their effects~~ on our ~~the~~ precipitation and water vapor isotopic ~~composition of~~data ~~vapor and precipitation~~ can be clearly

visualized on the ΔdΔδ-diagram. In ~~Xi'an~~this study, the below-cloud evaporation is the main process during the raindrops falling. However, ~~Snowfall~~ snowfall samples are less influenced by ~~the below-cloud processes~~the evaporation, and mainly preserve their initial water vapor information. ~~Hence, our results strengthen the reliability of using ice core to reconstruct the paleoclimate, paleoenvironment, and paleohydrology in the cold area.~~ The different Δd/Δδ slopes of rainfall and snowfall ~~may~~ might be related to the precipitation types.

3. By comparing the two methods, we find that both could be used to quantitatively evaluate the below-cloud evaporation effect, because there are no statistic differences on their $\Delta\delta^2H_p$ results. The slope of $F_i/\Delta\delta^2H$ in method 1 (1.00 ‰/%) is a little steeper than in method 2 (0.91 ‰/%), indicating the stronger evaporation effect on $\Delta\delta^2H$ for method 1. However, the two methods of $\Delta\delta^2H$ show large difference in winter, especially for snow samples, which is related to supersaturation process that is not considered in method 1. Through meteorology and sensitivity analysis, RH is the main controlling factor. The two methods show different sensitivity on temperature variations. Through uncertainty estimations, the method 2 show larger uncertainty range (ranging from 0.60 to 1.05‰) than the method 1 (ranging from 0.71 to 0.72‰).

~~Compared with the isotopic method, the evaporation rate computed by the mass conservation model is overestimated. The relative humidity is the main controlling factor in computing the remaining fraction of raindrops below-cloud evaporation. Due to more uncertain parameters in the mass conservation model, such as raindrop diameter, evaporation intensity, raindrop falling velocity, and no consideration of precipitation type, it is more suitable to use the isotopic model to calculate the remaining fraction of evaporated raindrops.~~

~~4. In Xi'an, the evaporation rates are higher in spring and summer, and lower in autumn and winter, and this is related to the variation of local RH.~~

Data availability

The datasets can be obtained from the TableS1.

Author contribution

Meng Xing and Weiguo Liu designed the experiments, interpreted the results, and

prepared the manuscript with contributions from all co-authors. Meng Xing and Jing Hu analyzed the precipitation and water vapor samples. Jing Hu maintained the experimental instruments.

Competing interests

The authors declare that they have no conflict of interest.

Acknowledgment

This work was supported by Science Foundation of China (No. 42177093), West Light Foundation of The Chinese Academy of Sciences, and China scholarship council. The authors would like to thank Mr. Xijing Cao for helping to collect precipitation samples.

References

Aemisegger, F., Sturm, P., Graf, P., Sodemann, H., Pfahl, S., Knohl, A. and Wernli, H.: Measuring variations of δ 18O and δ 2H in atmospheric water vapour using two commercial laser-based spectrometers: An instrument characterisation study, Atmos. Meas. Tech., 5(7), 1491–1511, doi:10.5194/amt-5-1491-2012, 2012.

Araguás-Araguás, L., Froehlich, K. and Rozanski, K.: Deuterium and oxygen-18 isotope composition of precipitation and atmospheric moisture, Hydrol. Process., 14(8), 1341–1355, doi:10.1002/1099-1085(20000615)14:8<1341::AID-HYP983>3.3.CO;2-Q, 2000.

Bastrikov, V., Steen-Larsen, H. C., Masson-Delmotte, V., Gribanov, K., Cattani, O., Jouzel, J. and Zakharov, V.: Continuous measurements of atmospheric water vapour isotopes in western Siberia (Kourovka), Atmos. Meas. Tech., 7(6), 1763–1776, doi:10.5194/amt-7-1763-2014, 2014.

Benetti, M., Reverdin, G., Pierre, C., Merlivat, L., Risi, C., Steen-Larsen, H. C. and Vimeux, F.: Deuterium excess in marine water vapor: Dependency on relative humidity and surface wind speed during evaporation, J. Geophys. Res., 119(2), 584–593, doi:10.1002/2013JD020535, 2014.

Bowen, G. J., Cai, Z., Fiorella, R. P. and Putman, A. L.: Isotopes in the Water Cycle: Regional- to Global-Scale Patterns and Applications, Annu. Rev. Earth Planet. Sci., 47(1), 453–479, doi:10.1146/annurev-earth-053018-060220, 2019.

Cai, Y., Cheng, H., An, Z., Edwards, R. L., Wang, X., Tan, L. and Wang, J.: Large variations of oxygen isotopes in precipitation over south-central Tibet during Marine Isotope Stage 5, Geology, 38(3), 243–246, doi:10.1130/G30306.1, 2010.

Chakraborty, S., Sinha, N., Chattopadhyay, R., Sengupta, S., Mohan, P. M. and Datye, A.: Atmospheric controls on the precipitation isotopes over the Andaman Islands, Bay of Bengal,

Sci. Rep., 6, 19555 [online] Available from: https://doi.org/10.1038/srep19555, 2016.
Christner, E., Aemisegger, F., Pfahl, S., Werner, M., Cauquoin, A., Schneider, M., Hase, F., Barthlott, S. and Schädler, G.: The Climatological Impacts of Continental Surface Evaporation, Rainout, and Subcloud Processes on δD of Water Vapor and Precipitation in Europe, J. Geophys. Res. Atmos., 123(8), 4390–4409, doi:10.1002/2017JD027260, 2018.
Clark, I. D. and Fritz, P.: Environmental Isotopes in Hydrogeology, Lewis, Boca Raton, Florida., 1997.
Craig, H.: Isotopic Variations in Meteoric Waters, Science (80-.)., 133(3465), 1702–1703, 1961.
Dansgaard, W.: Stable isotopes in precipitation, Tellus, 16(4), 436–468, doi:10.3402/tellusa.v16i4.8993, 1964.
Deshpande, R. D., Maurya, A. S., Kumar, B., Sarkar, A. and Gupta, S. K.: Rain-vapor interaction and vapor source identification using stable isotopes from semiarid western India, J. Geophys. Res. Atmos., 115(23), 1–11, doi:10.1029/2010JD014458, 2010.
Fiorella, R. P., Bares, R., Lin, J. C., Ehleringer, J. R. and Bowen, G. J.: Detection and variability of combustion-derived vapor in an urban basin, Atmos. Chem. Phys., 18(12), 8529–8547, doi:10.5194/acp-18-8529-2018, 2018.
Froehlich, K., Kralik, M., Papesch, W., Rank, D., Scheifinger, H. and Stichler, W.: Deuterium excess in precipitation of Alpine regions – moisture recycling, Isotopes Environ. Health Stud., 44(1), 61–70, doi:10.1080/10256010801887208, 2008.
Gat, J. R.: OXYGEN AND HYDROGEN ISOTOPES IN THE HYDROLOGIC CYCLE, Annu. Rev. Earth Planet. Sci., 24(1), 225–262, doi:10.1146/annurev.earth.24.1.225, 1996.
Gorski, G., Strong, C., Good, S. P., Bares, R., Ehleringer, J. R. and Bowen, G. J.: Vapor hydrogen and oxygen isotopes reflect water of combustion in the urban atmosphere, Proc. Natl. Acad. Sci., 112(11), 3247–3252, doi:10.1073/pnas.1424728112, 2015.
Graf, P., Wernli, H., Pfahl, S. and Sodemann, H.: A new interpretative framework for below-cloud effects on stable water isotopes in vapour and rain, Atmos. Chem. Phys., 19(2), 747–765, doi:10.5194/acp-19-747-2019, 2019.
Guan, H., Zhang, X., Skrzypek, G., Sun, Z. and Xu, X.: Deuterium excess variations of rainfall events in a coastal area of south Australia and its relationship with synoptic weather systems and atmospheric moisture sources, J. Geophys. Res. Atmos., 118(2), 1123–1138, doi:10.1002/jgrd.50137, 2013.
Jacob, H. and Sonntag, C.: An 8-year record of the seasonal variation of 2 H and 18 O in atmospheric water vapour and precipitation at Heidelberg, Germany, Tellus B Chem. Phys. Meteorol., 43(3), 291–300, doi:10.3402/tellusb.v43i3.15276, 1991.
Jeelani, G., Deshpande, R. D., Galkowski, M. and Rozanski, K.: Isotopic composition of daily precipitation along the southern foothills of the Himalayas: Impact of marine and continental sources of atmospheric moisture, Atmos. Chem. Phys., 18(12), 8789–8805, doi:10.5194/acp-18-8789-2018, 2018.
Jouzel, J. and Merlivat, L.: Deuterium and oxygen 18 in precipitation: Modeling of the isotopic effects during snow formation, J. Geophys. Res., 89(D7), 11749, doi:10.1029/jd089id07p11749,

1984.
Jouzel, J., Delaygue, G., Landais, A., Masson-Delmotte, V., Risi, C. and Vimeux, F.: Water isotopes as tools to document oceanic sources of precipitation, Water Resour. Res., 49(11), 7469–7486, doi:https://doi.org/10.1002/2013WR013508, 2013.
Li, L. and Garzione, C. N.: Spatial distribution and controlling factors of stable isotopes in meteoric waters on the Tibetan Plateau : Implications for paleoelevation reconstruction, Earth Planet. Sci. Lett., 460, 302–314, doi:10.1016/j.epsl.2016.11.046, 2017.
Li, Z., Qi, F., Wang, Q. J., Kong, Y., Cheng, A., Song, Y., Li, Y., Li, J. and Guo, X.: Contributions of local terrestrial evaporation and transpiration to precipitation using δ 18 O and D-excess as a proxy in Shiyang inland river basin in China, Glob. Planet. Chang., 146, 140–151, 2016.
Liu, W., Feng, X., Liu, Y., Zhang, Q. and An, Z.: δ18O values of tree rings as a proxy of monsoon precipitation in arid Northwest China, Chem. Geol., 206(1), 73–80, doi:https://doi.org/10.1016/j.chemgeo.2004.01.010, 2004.
Liu, W., Liu, H., Wang, Z., An, Z. and Cao, Y.: Hydrogen isotopic compositions of long-chain leaf wax n-alkanes in Lake Qinghai sediments record palaeohydrological variations during the past 12 ka, Quat. Int., 449, 67–74, doi:https://doi.org/10.1016/j.quaint.2017.05.024, 2017a.
Liu, W., Wang, H., Leng, Q., Liu, H., Zhang, H. and Xing, M.: Hydrogen isotopic compositions along a precipitation gradient of Chinese Loess Plateau : Critical roles of precipitation / evaporation and vegetation change as controls for leaf wax δ D, Chem. Geol., 528(April), 119278, doi:10.1016/j.chemgeo.2019.119278, 2019.
Liu, Y., Liu, H., Song, H., Li, Q., Burr, G. S., Wang, L. and Hu, S.: A monsoon-related 174-year relative humidity record from tree-ring δ18O in the Yaoshan region, eastern central China, Sci. Total Environ., 593–594, 523–534, doi:https://doi.org/10.1016/j.scitotenv.2017.03.198, 2017b.
Peng, T. R., Liu, K. K., Wang, C. H. and Chuang, K. H.: A water isotope approach to assessing moisture recycling in the island-based precipitation of Taiwan: A case study in the western Pacific, Water Resour. Res., 47(8), 1–11, doi:10.1029/2010WR009890, 2011.
Putman, A. L., Fiorella, R. P., Bowen, G. J. and Cai, Z.: A Global Perspective on Local Meteoric Water Lines-SM, Water Resour. Res., 1–6, doi:10.1351/pac198961081483.Jaffey, 2019a.
Putman, A. L., Fiorella, R. P., Bowen, G. J. and Cai, Z.: A Global Perspective on Local Meteoric Water Lines: Meta-analytic Insight into Fundamental Controls and Practical Constraints, Water Resour. Res., 2019WR025181, doi:10.1029/2019WR025181, 2019b.
Rangarajan, R., Laskar, A. H., Bhattacharya, S. K., Shen, C. C. and Liang, M. C.: An insight into the western Pacific wintertime moisture sources using dual water vapor isotopes, J. Hydrol., 547, 111–123, doi:10.1016/j.jhydrol.2017.01.047, 2017.
Salamalikis, V., Argiriou, A. A. and Dotsika, E.: Isotopic modeling of the sub-cloud evaporation effect in precipitation, Sci. Total Environ., 544, 1059–1072, doi:10.1016/j.scitotenv.2015.11.072, 2016.
Salmon, O. E., Welp, L. R., Baldwin, M. E., Hajny, K. D., Stirm, B. H. and Shepson, P. B.: Vertical profile observations of water vapor deuterium excess in the lower troposphere, Atmos. Chem. Phys., 19(17), 11525–11543, doi:10.5194/acp-19-11525-2019, 2019.

Steen-Larsen, H. C., Johnsen, S. J., Masson-Delmotte, V., Stenni, B., Risi, C., Sodemann, H., Balslev-Clausen, D., Blunier, T., Dahl-Jensen, D., Ellehøj, M. D., Falourd, S., Grindsted, A., Gkinis, V., Jouzel, J., Popp, T., Sheldon, S., Simonsen, S. B., Sjolte, J., Steffensen, J. P., Sperlich, P., Sveinbjörnsdóttir, A. E., Vinther, B. M. and White, J. W. C.: Continuous monitoring of summer surface water vapor isotopic composition above the Greenland Ice Sheet, Atmos. Chem. Phys., 13(9), 4815–4828, doi:10.5194/acp-13-4815-2013, 2013.

Stewart, M. K.: Stable isotope fractionation due to evaporation and isotopic exchange of falling waterdrops: Applications to atmospheric processes and evaporation of lakes, J. Geophys. Res., 80(9), 1133–1146, doi:10.1029/JC080i009p01133, 1975.

Sun, C., Chen, W., Chen, Y. and Cai, Z.: Stable isotopes of atmospheric precipitation and its environmental drivers in the Eastern Chinese Loess Plateau , China, J. Hydrol., 581(November 2019), 124404, doi:10.1016/j.jhydrol.2019.124404, 2020.

Tan, L., An, Z., Huh, C.-A., Cai, Y., Shen, C.-C., Shiau, L.-J., Yan, L., Cheng, H. and Edwards, R. L.: Cyclic precipitation variation on the western Loess Plateau of China during the past four centuries, Sci. Rep., 4(1), 6381, doi:10.1038/srep06381, 2014.

Thompson, L. G., Yao, T., Mosley-Thompson, E., Davis, M. E., Henderson, K. A. and Lin, P.-N.: A High-Resolution Millennial Record of the South Asian Monsoon from Himalayan Ice Cores, Science (80-.)., 289(5486), 1916 LP – 1919, doi:10.1126/science.289.5486.1916, 2000.

Tian, C., Wang, L., Kaseke, K. F. and Bird, B. W.: Stable isotope compositions (δ 2 H , δ 18 O and δ 17 O) of rainfall and snowfall in the central United States, Sci. Rep., (October 2017), 1–15, doi:10.1038/s41598-018-25102-7, 2018.

Wan, H., Liu, W. and Xing, M.: Isotopic composition of atmospheric precipitation and its tracing significance in the Laohequ Basin, Loess plateau, China, Sci. Total Environ., 640–641(May), 989–996, doi:10.1016/j.scitotenv.2018.05.338, 2018.

Wang, S., Zhang, M., Che, Y., Chen, F. and Fang, Q.: Contribution of recycled moisture to precipitation in oases of arid central Asia: A stable isotope approach, Water Resour. Res., 52(4), 3246–3257, doi:10.1002/2015WR018135, 2016a.

Wang, S., Zhang, M., Che, Y., Zhu, X. and Liu, X.: Influence of Below-Cloud Evaporation on Deuterium Excess in Precipitation of Arid Central Asia and Its Meteorological Controls, J. Hydrometeorol., 17(7), 1973–1984, doi:10.1175/JHM-D-15-0203.1, 2016b.

Wang, S., Zhang, M., Hughes, C. E., Crawford, J., Wang, G., Chen, F., Du, M., Qiu, X. and Zhou, S.: Meteoric water lines in arid Central Asia using event-based and monthly data, J. Hydrol., 562(May), 435–445, doi:10.1016/j.jhydrol.2018.05.034, 2018a.

Wang, Z., An, Z., Liu, Z., Qiang, X., Zhang, F. and Liu, W.: Hydroclimatic variability in loess δDwax records from the central Chinese Loess Plateau over the past 250 ka, J. Asian Earth Sci., 155, 49–57, doi:https://doi.org/10.1016/j.jseaes.2017.11.008, 2018b.

Welp, L. R., Lee, X., Kim, K., Griffis, T. J., Billmark, K. A. and Baker, J. M.: δ18O of water vapour, evapotranspiration and the sites of leaf water evaporation in a soybean canopy, Plant, Cell Environ., 31(9), 1214–1228, doi:10.1111/j.1365-3040.2008.01826.x, 2008.

Wu, J., Li, P. and Qian, H.: Variation characteristics of meteorological elements and prediction

model of available precipitation in Xi'an city, South-to-North water Transf. water Sci. Technol., 11(001), 50–54, 2013.

Xing, M., Liu, W., Li, X., Zhou, W., Wang, Q., Tian, J., Li, X., Tie, X., Li, G., Cao, J., Bao, H. and An, Z.: Vapor isotopic evidence for the worsening of winter air quality by anthropogenic combustion-derived water, Proc. Natl. Acad. Sci., 117(52), 33005–33010, doi:10.1073/pnas.1922840117, 2020.

Yao, T., Thompson, L. G., Mosley-Thompson, E., Zhihong, Y., Xingping, Z. and Lin, P.-N.: Climatological significance of δ18O in north Tibetan ice cores, J. Geophys. Res. Atmos., 101(D23), 29531–29537, doi:10.1029/96JD02683, 1996.

Yao, T., Masson-Delmotte, V., Gao, J., Yu, W., Yang, X., Risi, C., Sturm, C., Werner, M., Zhao, H., He, Y., Ren, W., Tian, L., Shi, C. and Hou, S.: A review of climatic controls on δ18O in precipitation over the Tibetan Plateau: Observations and simulations, Rev. Geophys., 51(4), 525–548, doi:10.1002/rog.20023, 2013.

Zhao, L., Liu, X., Wang, N., Kong, Y., Song, Y., He, Z., Liu, Q. and Wang, L.: Contribution of recycled moisture to local precipitation in the inland Heihe River Basin, Agric. For. Meteorol., 271(July 2018), 316–335, doi:10.1016/j.agrformet.2019.03.014, 2019.

Zhu, G. F., Li, J. F., Shi, P. J., He, Y. Q., Cai, A., Tong, H. L., Liu, Y. F. and Yang, L.: Relationship between sub-cloud secondary evaporation and stable isotope in precipitation in different regions of China, Environ. Earth Sci., 75(10), 876, 2016.